Acta Pharmaceutica Sinica B 2023;13(7):2844–2876

Chinese Pharmaceutical Association
Institute of Materia Medica, Chinese Academy of Medical Sciences

Acta Pharmaceutica Sinica B

www.elsevier.com/locate/apsb
www.sciencedirect.com

REVIEW

Phototriggered structures: Latest advances in biomedical applications

Mojtaba Shamsipur*, Atefeh Ghavidast*, Afshin Pashabadi

Department of Chemistry, Razi University, Kermanshah 6714414971, Iran

Received 1 January 2023; received in revised form 12 March 2023; accepted 11 April 2023

KEY WORDS

Phototrigger;
Light irradiation;
Excited state proton transfer;
Drug delivery system;
Dynamic process;
Controlling chemistry

Abstract Non-invasive control of the drug molecules accessibility is a key issue in improving diagnostic and therapeutic procedures. Some studies have explored the spatiotemporal control by light as a peripheral stimulus. Phototriggered drug delivery systems (PTDDSs) have received interest in the past decade among biological researchers due to their capability the control drug release. To this end, a wide range of phototrigger molecular structures participated in the DDSs to serve additional efficiency and a high-conversion release of active fragments under light irradiation. Up to now, several categories of PTDDSs have been extended to upgrade the performance of controlled delivery of therapeutic agents based on well-known phototrigger molecular structures like *o*-nitrobenzyl, coumarinyl, anthracenyl, quinolinyl, *o*-hydroxycinnamate and hydroxyphenacyl, where either of one endows an exclusive feature and distinct mechanistic approach. This review conveys the design, photochemical properties and essential mechanism of the most important phototriggered structures for the release of single and dual (similar or different) active molecules that have the ability to quickly reason of the large variety of dynamic biological phenomena for biomedical applications like photo-regulated drug release, synergistic outcomes, real-time monitoring, and biocompatibility potential.

*Corresponding authors.
E-mail addresses: mshamsipur@yahoo.com (Mojtaba Shamsipur), at.ghavidast@yahoo.com (Atefeh Ghavidast).

Peer review under the responsibility of Chinese Pharmaceutical Association and Institute of Materia Medica, Chinese Academy of Medical Sciences.

https://doi.org/10.1016/j.apsb.2023.04.005

1. Introduction

Over the past decade, special and great regard has been paid to the combination of the stimuli-triggered molecules with active biomaterial owing to multiple advantages in human healthcare such as controlled delivery of diagnostic, regulated drug delivery, therapeutic and pharmaceutical factors[1−6]. The triggered molecules are defined as the units, which can change their structure due to isomerization, dimerization or bond cleavage in response to an external stimulus for the release of active molecules[7−13]. Living organisms in nature are rich in examples that can reversibly regulate their configuration and properties in response to environmental stimuli. Heat-shock transformation in bacteria[14], camouflage in chameleons[15] and color changes in echinoderms in response to light[16] are wide ranging instances for this. Such triggered materials with the ability of responding to stimulus are considered to be an important class of advanced materials that can be utilized in biomedical applications and nanomedicine, particularly in the development of stimuli-triggered drug delivery systems (DDSs)[17−28].

So far, several external stimuli have been developed, such as light[29−35], temperature[36−38], magnetism[39−42], ultrasound[43,44] and electricity[45]. Among the mentioned external stimuli, light stimulation has attracted exceptional attention due to its ease of application without chemical contaminants, high spatial resolution, noninvasive nature and exact temporal and spatial control[29,46−51]. Wider ranges of the light wavelengths from ultraviolet (UV, λ_{max} = 200−400 nm) to visible (Vis, λ_{max} = 400−750 nm) or near-infrared (NIR, λ_{max} = 750−2000 nm) can be employed to trigger photo-sensitivity. Compared to UV and visible light, NIR light has less photo-toxicity, better tissues penetration depth and reduced background signal for biological applications. However, the application of NIR light is restricted due to its long wavelength, which has not enough energy to disrupt of chemical structures through bond-breaking or conformation-switching to triggered DDSs[52−55]. Recently, this issue solved by two-photon actuation (Section 3.1.1) in the range of 650−900 nm or upconversion NPs (UCNPs) technologies[56]. In comparison, UV light is a somewhat inferior nominee due to its toxicity under prolonged treatment and poor tissue penetration capacities (around 10 mm) due to light scattering and absorbance by intrinsic biological chromophores[57,58]. However, attempts have been provided to address these restrictions by a micro-light (MLight) source that can be implanted locally inside the human body[59,60]. In contrast, visible light can lead minor damage than UV light in vivid systems that has been recommended as an alternative to phototriggered DDSs (PTDDSs)[61].

Phototriggers, also known as photo-removable protecting groups (PRPG), undergo an irreversible dissociation by selectively breaking a chemical bond can release leaving groups (LG) as bioactive molecules at specific time under light irradiation (Fig. 1)[62]. Therefore, a PTDDS can distribute a bioactive agent upon a specific wavelength light instantly at the preferred place in instant to attain a focused high value of drug while reducing generally injected dosage level and total poisonous effects as a result of their non-invasiveness and spatiotemporal accuracy[63]. This proves greatly assure for drugs with adverse toxicity and side-effects or for targeted therapy efficiency of them. With increasing applications of light-responsive DDSs particularly in biomedical applications, new improvements of phototriggers are needed to fulfill the requirements for better sensitivity, low toxicity, structural simplicity, desirable solubility in the targeted

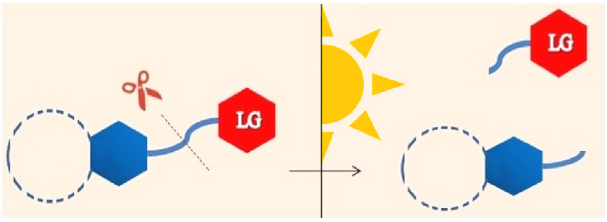

Figure 1 The general representative of phototriggered molecules.

media, faster kinetics, effective fluorescence embodiment and an adjustable and strong absorption spectrum above 300 nm. So far, several phototriggers such as *o*-nitrobenzyl (ONB)[64,65], coumarin[66,67], *p*-hydroxylphenacyl (*p*HP)[68,69], hydroxycinnmate[70,71], benzoin (Bnz)[72−74], nitroindoline (NI)[75−77] and 8-bromo-7-hydroxylquinoline (BHQ)[78,79] have been applied in DDS during the past decade.

To date, to further improvement the therapeutic results and reduce side effects, integration of nanotechnology with phototriggered molecules has opened new horizons for synergistic therapies[25]. Nano-platforms such as polymeric nanoparticles (NPs), liposomes, metal−organic cages and metallic NPs have provided a complementary means for delivery of therapeutic agents into diseased cells and tissues using safe and effective directions[80−85]. In this review, we will focus on latest developments of conventional phototriggers to provide more effective therapies against serious illnesses with reduced the damage to healthy cells and open new perspective toward favorable bioavailability and drug delivery efficiency.

2. Phototriggered drug delivery systems (PTDDSs)

PTDDSs facilitate the release of LGs such as therapeutic agents or drug cargos through different mechanisms including bond cleavage[86−89], isomerization[90−92], photo-oxidation[93,94], photoreduction[95,96], cross-linking[97,98] and photocaging/uncaging[99,100], by light irradiation. These transformations can be caused disruption and dissociation of extant structures or even altering the lower critical solution temperature (LCST) transition[8,101,102]. Here, we discuss important latest advances on phototriggered molecules together with their essential mechanisms and their conditions for stimulation based on two types of light-induced drug release. One is the direct release of the drug as a LG by photochemical bond cleavage of *p*-hydroxyphenacyl (*p*HP), *o*-hydroxycinnamate, tetraphenylethylene (TPE), and coumarin substituted and the other is the photoinduced disruption of nanoscale structures such as micelles and MOCs having nitroaryl derivatives, thioketal, maleimide-anthracene, spiropyranes (SP) and azobenzenes (Azo) moiety to release the drug cargo. In addition, the dual-releasing phototriggers as a novel combination therapy with the ability to release two anticancer drugs are discussed at the end of review (Fig. 2).

3. PTDDSs based on photochemical bond cleavage

The photochemical bond cleavage strategy assists intramolecular self-immolation to the release of the bioactive molecules such as enzymes, neurotransmitters, cell-signaling molecules, fluorophores, fragrances and drugs on a particular site with exact control of their dosages using light irradiation length[86,103]. The

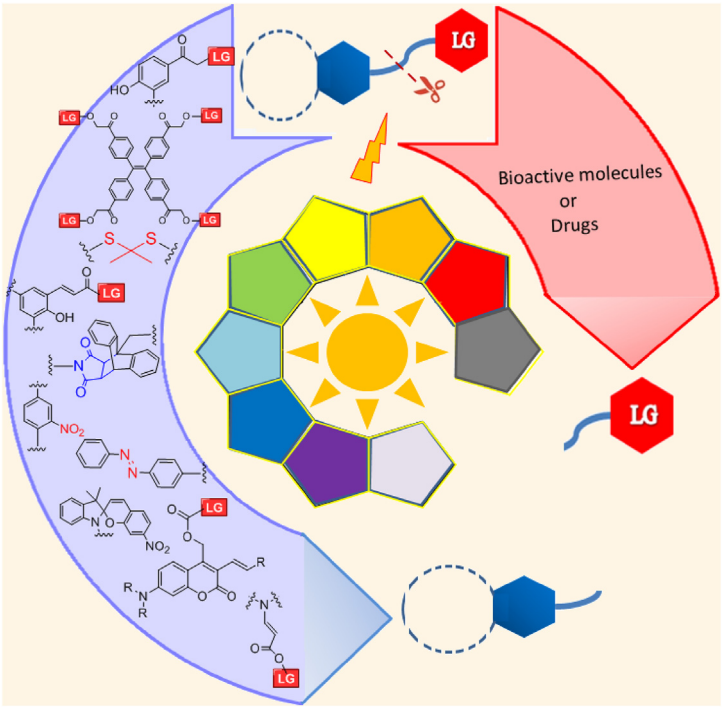

Figure 2 Schematic illustration of PTDDSs.

*p*HP, *o*-hydroxycinnamate, nitroaryl, TPE, and coumarin derivatives are good examples for these purposes, which noticed as a critical step for biomedical applications of phototriggers.

3.1. *p-Hydroxyphenacyl*

The *p*HP groups are good phototrigger example for the study of very fast biological procedures with high photochemical quantum yield[104–106], however, due to non-fluorescent behavior and excitation wavelength below 400 nm, *p*HP group receives less attention as a delivery agent[107]. To overcome these issues, Barman et al.[108] have incorporated 2-(2′-hydroxyphenyl)benzothiazole (HBT) moiety to *p*HP derivative toward the design a photo-induced DDS, entitled *p*-hydroxyphenacyl-benzothiazole-chlorambucil (*p*HP-Benz-Cbl), see Scheme 1.

First, the salicylaldehyde **1** transformed to derivative **3** using Friedel–Crafts acylation and treated with the anticancer drug chlorambucil (Cbl) to afford **4**. Afterward, the treatment of **4** with 2-aminothiophenol **5** yielded the *p*HP-Benz-Cbl as excited-state intramolecular proton transfer (ESIPT)-assisted phototrigger for the very fast photorelease of Cbl inside the cell (15 min) using the visible wavelength (≥410 nm). Herein, the *p*HP group integration on the HBT caused a distinct fluorescence discolor from green to blue after photorelease and assisted in the deprotonation of *p*HP segment to accelerate the release process *via* ESIPT. Upon visible light irradiation, *p*HP-Benz-Cbl (with an intense green-emission band) excites to the singlet state undertakes a fast ESIPT, where a proton translocation occurs from the *p*HP to the benzo-thiazole segment, producing **7** and subsequently zwitterionic **8**. The intermediate **8** exceeds during proficient intersystem crossing (ISC) to triplet excited state that converts to a supposed spirodiketone **10** with the parallel release of the Cbl accompanied by a photo-Favorskii rearrangement. Finally, the hydrolytic ring opening of spirodiketone **10** yielded *p*HP-Benz-COOH **11** with an intense blue-emission band owing to conjugation disconnection from a phenolic hydroxy functional group to a carbonyl moiety. This phenomenon is obvious in emission spectrum (Fig. 3a) during 15 min. Fig. 3b–d, show the real-time monitoring of Cbl release by *p*HP-Benz-Cbl within malignant neoplastic disease tissue (MDA-MB 231). At first, the tissues have green fluorescence because of *p*HP-Benz-Cbl sorption (Fig. 3b, 0 min). After 10 min visible light irradiation with λ_{max} = 410 nm, two different green and blue fluorescence detected, signifying the Cbl incomplete release (Fig. 3c). In conclusion, after 15 min discolor from green to blue, suggesting a complete photorelease of Cbl drug and highest toxicity level (above 90%) toward cancer tissues (Fig. 3d).

Singh et al.[109] recently developed pHP based DDS with an excellent uncaging capacity in the area of 700 nm. Aggregation-induced-emission (AIE) chromophores have gained immense interest in biomedical purposes due to their unique possessions including exceptional photostability, excellent luminescence and biocompatibility[110–112]. In this way, they incorporated the naphthalene group into the *p*HP moiety so that a strong internal charge transfer occurred, causing in a red-shift in absorption bond and improved two-photon uncaging cross-section (Scheme 2). The prepared photo-induced DDS, *p*HP-Naph-Cbl exhibits exceptional properties like two-photon absorption in the phototherapeutic window (700 nm), high real-time monitoring ability due to a specific fluorescence color change from greenish-yellow to blue through the Cbl release and demonstrates AIE behavior, therefore remarkably releases the Cbl in the aggregated state with distinct fluorescence discolor.

3.1.1. *Two-photon excitation uncaging*

The two-photon excitation (2 PE) uncaging is a growing alternative method to evade the photo-toxicity of UV light and enhance spatial resolution *via* three-dimensional (3D) imaging in various fields, especially in cell biology[113–118]. This non-linear absorption

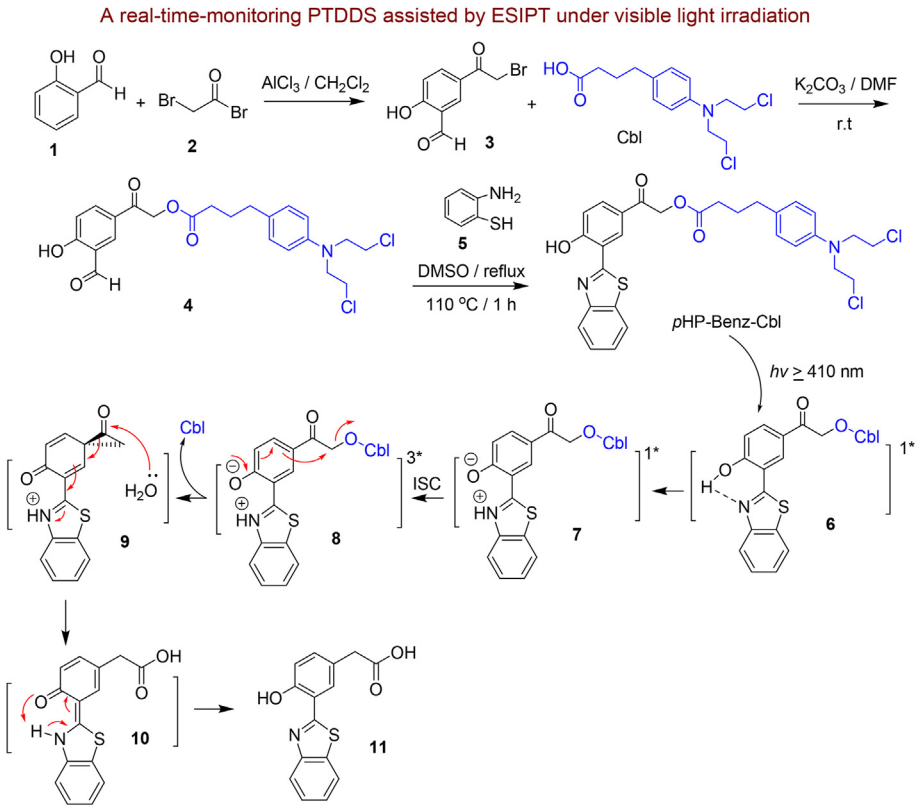

Scheme 1 Synthesis of the pHP-Benz-Cbl and its potential photorelease mechanism.

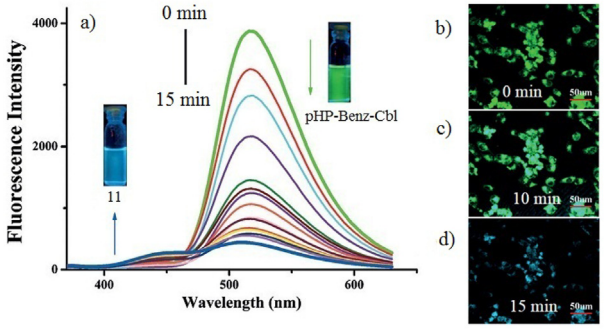

Figure 3 (a) Increase of emission spectra of *p*HP-Benz-Cbl during 0−15 min, and real-time monitoring of the Cbl liberation from *p*HP-Benz-Cbl during visible-light irradiation (b) 0 min, (c) 10 min and (d) 15 min by confocal microscopy. Reprinted with permission from Ref. 108. Copyright@2016 John Wiley & Sons, Inc.

occurrence can excite a molecule by simultaneous absorption of two photons with about half-energy instead of one, which doubles the corresponding irradiation wavelength compared with conventional one-photon excitation (1 PE). The phototrigger subsequently becomes red or NIR light, which their wavelengths can penetrate deeper into tumor cells and decrease the photodamage under treatment. Therefore, designing structures with two-photon photosensitivity is one of the most prevalent challenges in biomedical treatment. Recently, Klausen et al.[119] provide a systematically review to the explanation and design of two-photon phototriggered structures in uncaging of bioactive molecules.

3.2. *Tetraphenylethylene*

Among the various AIE chromophores, tetraphenyletheylene (TPE) and its analogs have achieved considerable importance in the field of cancer therapy mostly through their potential to perform as photosensitizers for photodynamic therapy (PDT) and cellular imaging[120,121]. The TPE derivatives are one of the ideal units for assembling macrocycles and cages due to its simple C_2 symmetry and as minimum tetratopic reaction situations[122,123]. To use the benefits of AIE and ESIPT combination, the Parthiban et al.[124] group developed a PTDDS using connection of TPE with *p*HP-Cbl (TPE-*p*HP-Cbl) that, released the Cbl only in their aggregated state under visible light ($\lambda \geq 410$ nm) irradiation with high real-time monitoring ability. This organized PTDDS due to its AIE phenomenon showed distinct fluorescence. Although, the visible light activated based on DDS by Barman et al.[108] and Parthiban et al.[124] did not display hopeful uncaging capacity in the area of 650−950 nm, which obstructs their sensible usage in the biomedical applications.

In the following, Parthiban et al.[125] synthesized for the first time a photo-induced nano-DDS with strong fluorescence by a TPE **13** functionalized with 4 equivalent Cbl as anticancer agent ($TPE(Cbl)_4$ NPs) (Scheme 3). The four-armed phototriggers $TPE(Cbl)_4$ was initially synthesized by Friedel−Crafts acylation and then reacted with Cbl. Subsequently, the $TPE(Cbl)_4$ NPs were synthesized by re-precipitation methods. They proved that 4 equiv of Cbl is librated in an ordinal procedure when the $TPE(Cbl)_4$ NPs induced by visible light through a C−O bond cleavage. Furthermore, $TPE(Cbl)_4$ and the released photoproducts exhibited a PDT property during drug release.

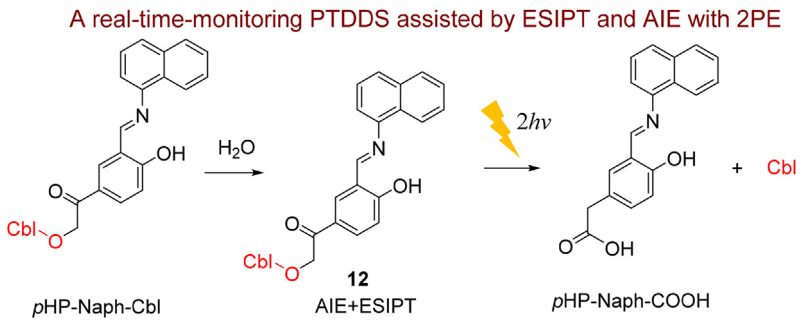

Scheme 2 Two-photon uncaging of *p*HP-Naph-Cbl.

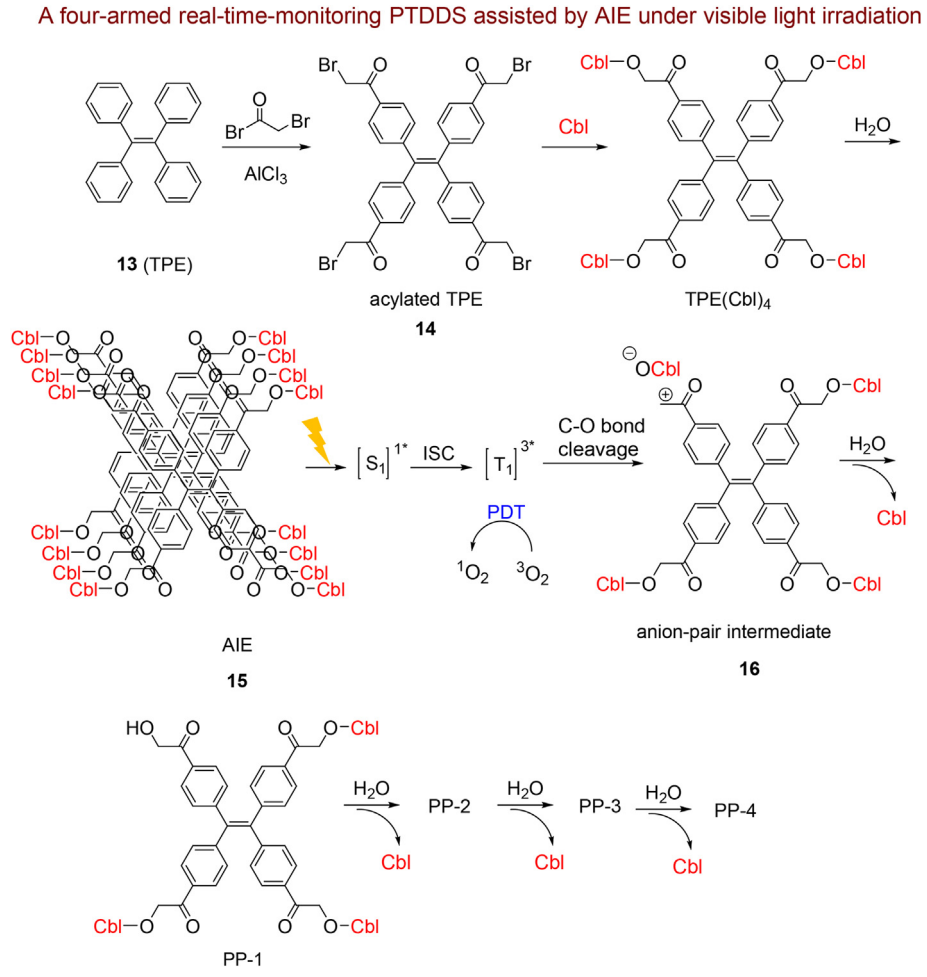

Scheme 3 Synthetic route and potential mechanism for produced singlet oxygen and sequential Cbl release.

Upon photolysis, $TPE(Cbl)_4$ NPs get excited to their singlet state and afterward to their triplet states through ISC. Then, $TPE(Cbl)_4$ NPs as a photosensitizer produce singlet oxygen and undergo heterolytic fission of the carbonate ester C−O bond to cause anion-pair intermediate **16**. After that, reaction of anion pair intermediate **16** with H_2O generated the photoproducts PP-1, PP-2, PP-3 and PP-4 sequentially, together with the ordinal Cbl release in their aggregated state. During cellular uptake, the cells exhibited a deep-green color due to existence of $TPE(Cbl)_4$ which has the AIE process capability (Fig. 4a). Upon 10 and 25 min visible irradiation, respectively (Fig. 4b and c), the amount of the fluorescence initially reduced and a weak green fluorescence observed that obviously signifies the breakup of $TPE(Cbl)_4$ NPs and disseminated Cbl inside the tumor cell. Incubation of tumor tissue (HeLa cell) with non-fluorescent dichlorodihydrofluorescein diacetate (DCFDA) and $TPE(Cbl)_4$ NPs displays weak green fluorescent (Fig. 4d) that after irradiation due to generation of a singlet oxygen through $TPE(Cbl)_4$ NP a strong green fluorescence observed (Fig. 4e and f). In fact, non-fluorescent DCFDA convert to green fluorescent dichlorofluorescein owing to oxidation by produced singlet oxygen species. Prominently, they confirmed that TPE functionalized with 4 equivalents of Cbl are very efficient

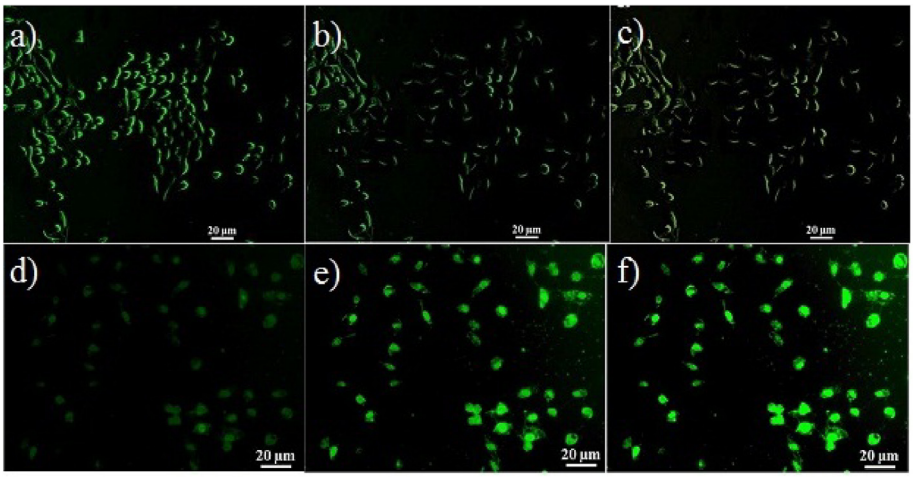

Figure 4 (a–c) Confocal microscopy representations of TPE(Cbl)$_4$ NPs in HeLa cell; (a) 0, (b) 10 and (c) 25 min irradiation, and (d–f) generation of a singlet oxygen *via* TPE(Cbl)$_4$ by DCFDA in HeLa cell; (d) 0, (e) 15 and (f) 25 min irradiation. Reprinted with permission from Ref. 125. Copyright@2019 American Chemical Society.

(lower 16% viability) compared to 1 equivalent of Cbl against cancer cells thanks to the synergistic effects of 4 equivalent of released Cbl and PDT activities.

In the other research work by the same group, they synthesized tetraphenylethylene conjugated *p*HP NPs (TPE-*p*HP-H_2S) for the controlled liberation of hydrogen sulfide (H_2S) upon exposure to visible light without the assistance of any peripheral reagent[126]. This H_2S donor triggered by light displays both AIE and ESIPT properties by TPE and pHP moieties, respectively. Furthermore, a real-time monitoring at the cellular level is possible with a simple fluorescence color change from yellow to green after photorelease.

3.3. *o-Hydroxycinnamate*

According to preceding considerations[127,128], Paul et al.[129] studied the application HBT as an ESIPT moiety in *o*-hydroxycinnamate fragment (HBT@*o*-hydroxycinnamate). As shown in Scheme 4, the authors designed the fluorescent phototrigger HBT@*o*-hydroxycinnamate by the attachment of HBT moiety to the *o*-hydroxycinnamate group for rapid and shortest release (60 min) of methyl salicylate **21** with distinct fluorescence color change from orange (because of the ESIPT occurrence) to blue (due to formed benzothiazole-coumarin **20**) following photorelease. The light-induced conversion of the (*E*)-photoisomer to the (*Z*)-photoisomer causes the release of alcohol in company with a coumarin as by-product (with intense fluorescent property and emission wavelength). The potent fluorescent of coumarin byproduct can be useful in the release of alcohol derivatives from these systems. Although, the limitation of this work is the phototrigger activates in the UV region (≥365 nm) as well as the strong chromophore benzothiazole-coumarin byproduct **20** operates as an optical filter.

3.4. *Coumarin substituted*

Among the synthetic phototriggers, coumarin-based derivatives as another important class of phototriggered molecules exhibit unique fluorescence visualization and liberate free drug molecules through a C–O bond breaking upon exposure light irradiation[102,130–134]. Accordingly, some researchers nominate a coumarin incorporated with heterocycle derivatives as the PTDD system for making the photo-induced release of antitumor agents[56,135,136]. In general, coumarins may be utilized both as a cross-linker and as a divisible moiety especially owing to their faster release rate compared to other phototriggered molecules such as ONB derivatives[137]. Coumarin functionalized at the 7-position with an electron-donating group (EDG) and at the 3-position with an electron-withdrawing group (EWG) display red-shifted absorption and emission in the blue-green light area (Scheme 5). The design of derivative **22** was a critical point burgeoning in the development of

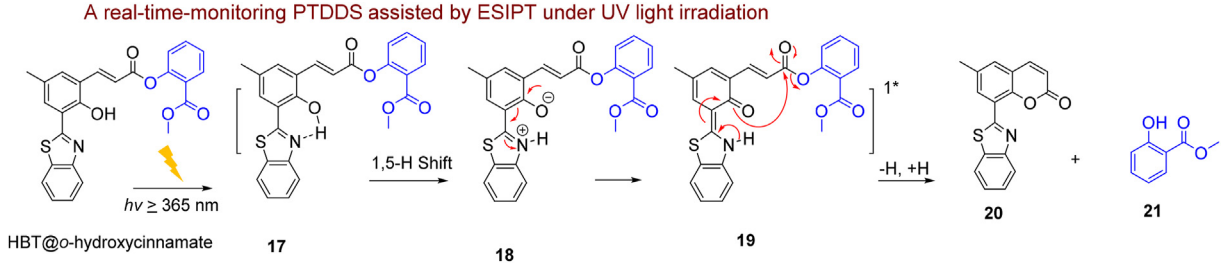

Scheme 4 Photoinduced uncaging of methyl salicylate **21** from compound HBT@*o*-hydroxycinnamate.

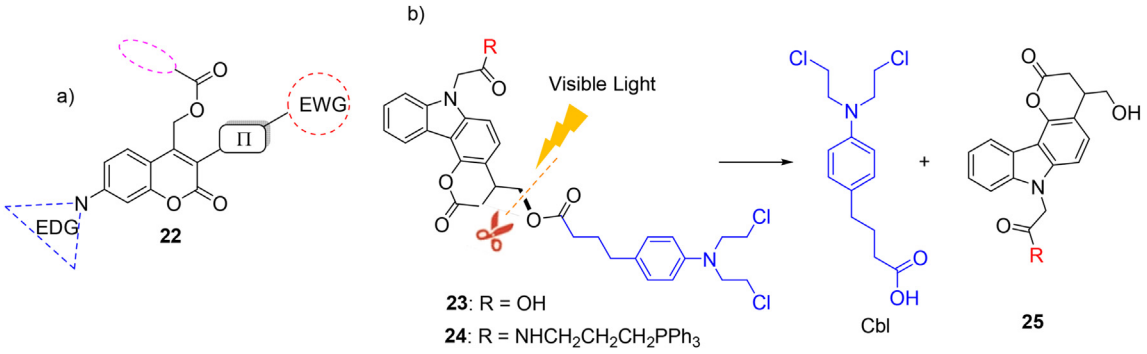

Scheme 5 Structures of (a) designed coumarin **22** and (b) a visible-light-triggered drug release of **23**, **24**.

cages for the biological and biomedical studies[138–143]. Wang et al.[144] examined the synthesis of two carbazole-coumarin derivatives **23** (with −COOH group) and **24** (with triphenylphosphonium (TPP) group) for the photocontrolled release of Cbl, in an *in vitro* model of cancer cells. The amine group of the carbazole moiety supplies as an EDG and the lactone segment of the coumarin serves as an EWG and permits the visible light of 405 nm to trigger the photodecomposition of the carbazole-coumarin-Cbl connection. Carbazole-coumarins **23** and **24** showed emission bands at 360 and 450 nm, correspondingly.

The photochemical release of Cbl drug is similar to what will be expressed later in Scheme 24[352]. Carbazole-coumarin **24** with the lower IC_{50} due to synergistic effect of chemo-drug strength and photosensitization proposed the high efficiency of the TPP structure in raising the bioavailability carbazole-coumarin-drug derivatives.

Klausen et al.[145] in other attempt attached an EWG and a π-conjugated linker through a vinyl-acceptor function at the 3-position of the coumarin, the respective results conveyed Fmoc-protected glycine release both at 700 and 900 nm. As already mentioned (Section 3.1.1), contrary to UV−visible light, the 2 PE by NIR wavelengths affords different benefits including profounder penetration in tumor cells, abridged photo-damage and inherent 3D resolution. A tiny collection of advanced dipolar coumarinylmethyl structure **26**−**31** that demonstrate great two-photon sensibility at two supplementary wavelengths in the NIR spectral area is illustrated in Scheme 6.

Further investigation revealed that the existence of the fused-ring on the EWG and most powerful EWG in the categories can intensify the photorelease efficiency. Therefore, compounds **26**−**28** are not proper for uncaging applications during C−O bond cleavage upon excitation. Meanwhile, a distinct performance examined for developed analogs **30** and **31** with a fluorenyl component in the conjugated π-connector.

Bojtar et al.[146] synthesized a click-and-release system based on coumarin with a supplementary degree of spatiotemporal manage for the liberation of the caged kinds (Scheme 7). They synthesized vinylene-linked coumarinyl-tetrazine **32** as a photocage that jointed with several amino acids including, Boc-phenylalanine, Fmoc-lysine and Boc-tyrosine-*t*Bu-ester as the model caged substrates. The presence of vinylene tetrazine moiety in the photocages **33**−**35** quenches the fluorescence of the coumarin moiety and they were fairly photostable and no liberation of the amino acids was perceived following blue laser lighting (λ_{max} = 488 nm).

However, fluorescence capability was changed upon altering the tetrazine **33**−**35** in a bioorthogonal reaction with bicyclo [6.1.0]non-4-yn-9-ylmethanol (BCN) **36**. Recently, bioorthogonal reactions allow researchers to label or manipulate biological systems in a single experiment[147–151]. The BCN-conjugated derivatives **37**−**39** demonstrated the most fluorescence (with a bright green-emission band) as well as the light-induced bond breaking to fast liberation of all three amino acids **44**−**46**. Fig. 5a and b clearly demonstrate that the live cells remediated alone with tetrazine derivative **47** demonstrated a tiny fluorescence growth while cells treated with TPP-BCN and then with **47** displayed bright yellow emission of coumarin **51** after irradiation (Fig. 5c and d). This can be due to the formation of BCN-conjugated derivative **48** caused by the bioorthogonal reaction of **47** with TPP-BCN according to Fig. 5e. The tetrazine derivative **47** have an excellent ability for uncaging monitoring process. Further, BCN with triphenylphosphonium moiety (TPP-BCN) used as a tiny organelle marker, to focus the bioorthogonal reaction into the mitochondria (Fig. 5e)[152].

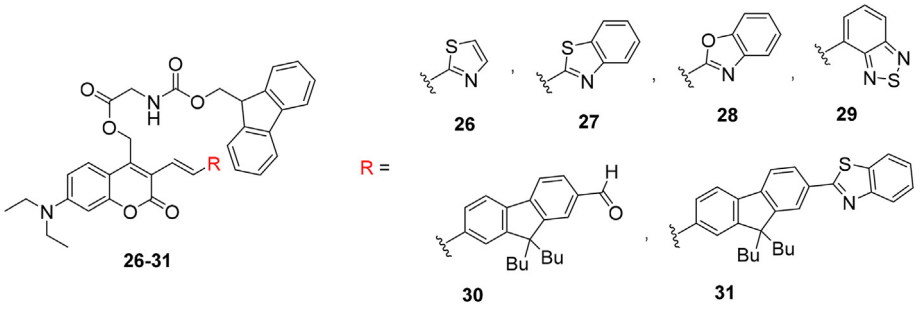

Scheme 6 Structures of π-extended coumarins **26**−**31**.

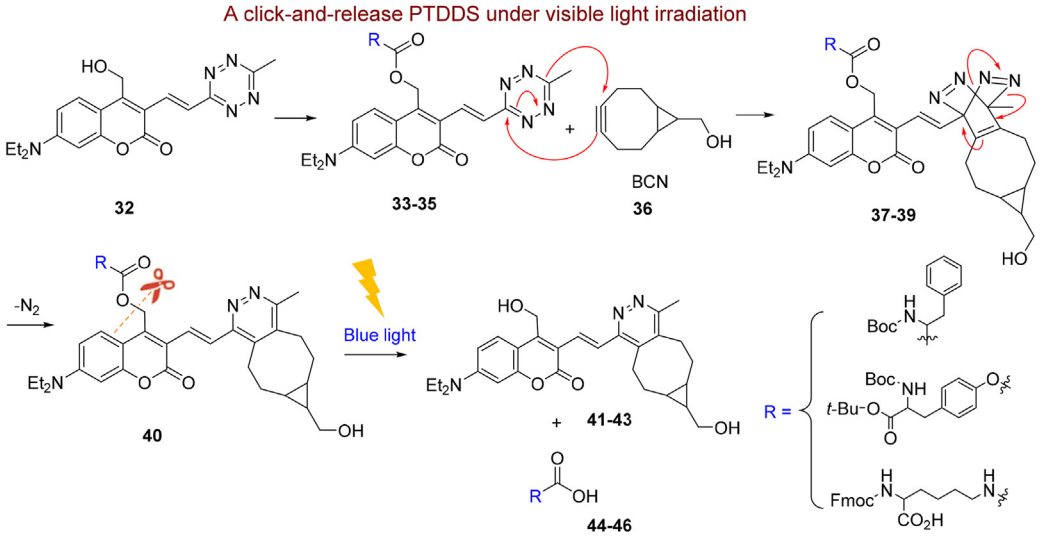

Scheme 7 Structure and conditional uncaging of the photocages.

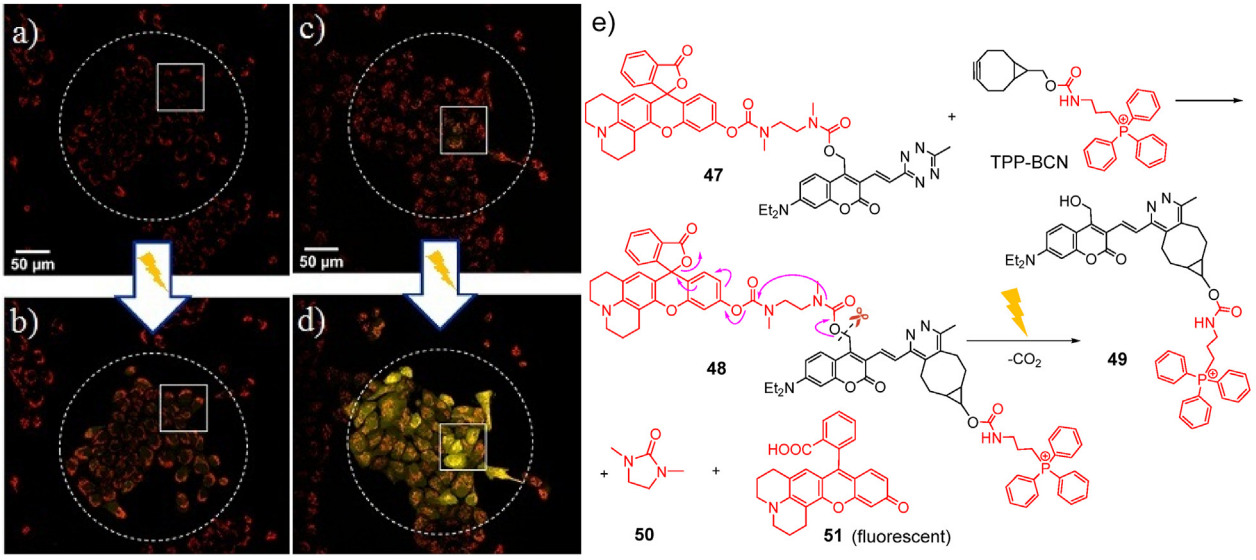

Figure 5 (a, b) Confocal images of tissues remediated alone with tetrazine derivative **47** (a) before and (b) after irradiation and (c, d) cells treated with TPP-BCN and then with **47** (c) before and (d) after irradiation and (e) reaction of tetrazine derivative **47** with TPP-BCN. Reprinted with permission from Ref. 146. Copyright@2020 American Chemical Society.

4. PTDDSs based on photoinduced disruption of nanoscale structures

4.1. Nitroaryl derivatives

Recently, nitroaryl derivatives including the ONB, *o*-nitro-2-phenethyl and *o*-nitro-anilide (ONA) groups used phototriggers to assemble photocages for the regulated liberation of important metallic ions, drugs or bioactive molecules[153–157]. In the ONB derivatives, an aci-nitro intermediate can form *via* an intramolecular hydrogen transfer to the nitro group (tautomerization) by irradiation. Despite their extensive applications, ONB photocages often show low quantum yield values (<0.05) owing to resonance stabilization of aci-nitro intermediates and their application is limited due to the highly absorbing and reactive side products[72,158]. A one photon blue visible light responsive polymeric carrier (up to 500 nm) based on ONB derivatives as a subcutaneously implanted depot developed by Carling et al.[159] and it has been used for medical cargo release in the hydrophobic microenvironments including the internal space of a polymeric particle. The improvement of one-photon visible photo-responsive structures represents an attractive alternative for *in vivo* applications due to very shorter lighting time period with lower powers consumption and is significantly less dangerous to the tissues than UV and NIR laser lights. In this work, to facilitate polymerization and enhance the kinetics of photo-degradation, the butanediol derivative 2-(4′-*N*-dimethylamino-4-nitro-[1,1′-biphenyl]-3-yl) butane-1,4-diyl dicarbonyl (ANBB) was firstly synthesized[160,161]

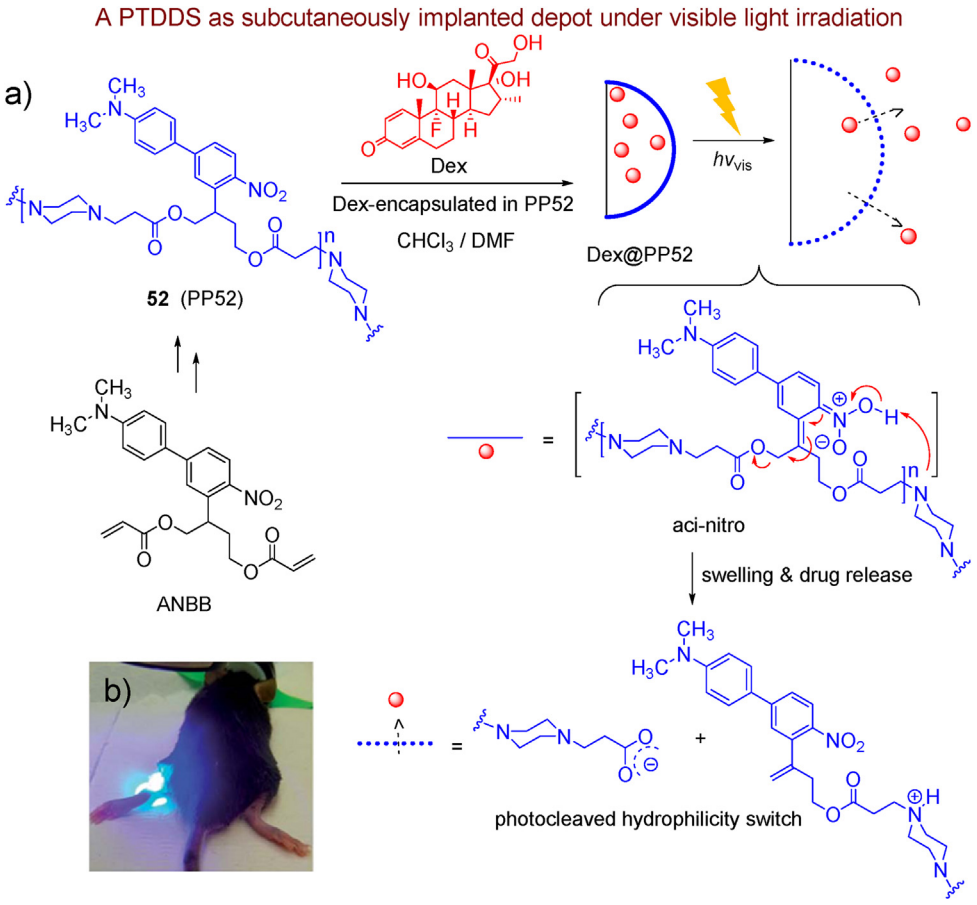

Scheme 8 (a) Schematic representative of Dex@PP52 and its swelling and Dex release under visible light irradiation and (b) *in vivo* photorelease of Dex@PP52 depot upon exposure to blue visible light. Reprinted with permission from Ref. 159. Copyright@2014 The Royal Society of Chemistry.

and then basic tertiary amine groups introduced in the polymer backbone for promotion photo-cleavage in hydrophobic environments (Scheme 8).

The tertiary amine functional group connected to photo-responsive polymer spine **46** (PP52) facilitate deprotonation of the aci-nitro intermediate directing to β-elimination and photo-cleavage according to Scheme 8. Therefore, the visible light irradiation of PP52 induces swelling and release of dexamethasone (Dex) as an anti-inflammatory agent *in vivo*. The therapeutic effects of Dex@PP52 were more effective than free Dex in local inflammation because of the release of Dex with greater efficiency in the target tissue, rapid diffusion and remaining as local depot on-demand at the injection site with minimizing adverse side effects. Dex@PP52 together with the NIR fluorescent probe IR780 permitted *in vivo* real-time monitoring of the depot release. Photograph Scheme 8b, demonstrates the *in vivo* photorelease of Dex@PP52 depot upon exposure to blue visible light. Advantages of this photo-responsive carrier were the strong visible light absorption above 500 nm and photo-reactivity in hydrophobic surroundings.

4.2. *Thioketal linkers*

4.2.1. *Reactive oxygen species-responsive thioketal carriers*

The irregular biochemical change of reactive oxygen species (ROS) level (lack/excess) in the disease sites can promote different diseases like autoimmune, cardiovascular, neurodegenerative and etc.[162–169]. This issue has motivated investigators to utilize imparity ROS amounts for creating ROS-responsive drug carriers. Thioketal, thioacetal, thioether, vinyldithioether, aryloxalate, selenium, tellurium and arylboronic esters linkers are effective ROS-cleavable chemical groups undergoing bond breaking upon treatment with ROS, therefore, have already been utilized to synthesis ROS-responsive DDSs[170–176]. Chen et al.[177] synthesized an amphiphilic and cationic ROS-responsive poly(β-amino ester) ($PBAE_{ROS}$) *via* insertion of a thioketal segment in its monomer unit to attain synergistic antitumor outcomes integrated with photothermal/photodynamic therapy (PTT/PDT) and chemotherapy treatment according to Scheme 9. Hereupon, $PBAE_{ROS}$ was used for load of photosensitizer IR780 (a near NIR dye, which has both intense PTT and PDT efficacies under laser illumination) and chemotherapeutic drug doxorubicin (DOX). Because the poly(β-amino ester) chains of $PBAE_{ROS}$ as hydrophobic moiety and side-chain hydroxyl groups as hydrophilic were conjugated, it was predictable that the poly(β-amino ester) chains and hydroxyl groups form a core/shell architecture in an aqueous medium, respectively. Nanomicelles of $PBAE_{ROS}$@IR780-DOX were prepared under stirring with dropwise addition of DOX and IR780 in DMSO and surface modification of polymer $PBAE_{ROS}$@IR780-DOX (PPID) was accomplished through propylene glycol alginate sodium sulfate (PSS) using an easy nanoprecipitation procedure (Scheme 9).

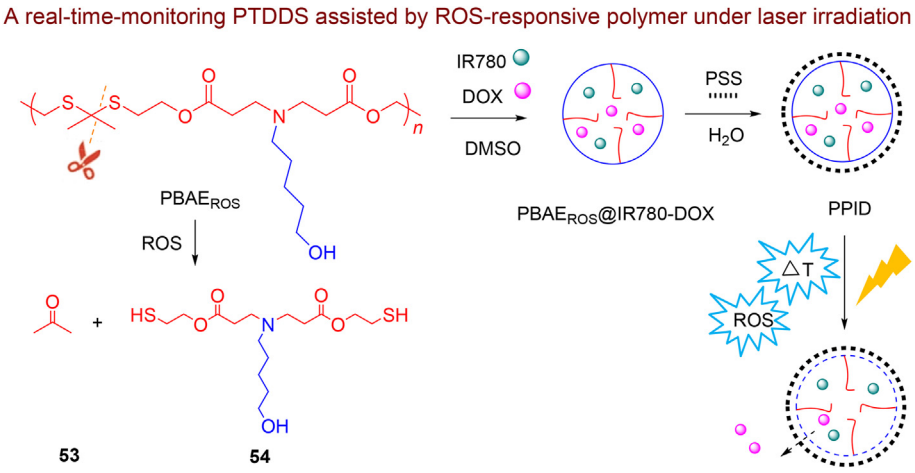

Scheme 9 Preparation of PPID NPs and their mechanisms *via* integrated with PTT/PDT and chemotherapy.

The positive charges on the surface of the PPID nanosystem facilitate the rapid penetration into the tumor tissues because of interplay with the negatively charged cell membranes. Upon exposure 808 nm laser light, PPID NPs cause a quick rise temperature and generated a wide range of cytotoxic ROS. The ROS generated by the IR780 advanced further breakage of the thioketal bonds and release of DOX, thereby synergistic PTT/PDT and chemotherapy efficiencies was observed *in vitro* photorelease. Further examinations unraveled the formation of by-products acetone **53** and dithiol **54** upon the cleavage of the thioketal bond of PBAEROS.

The fluorescence microscopic photographs of Hep1-6 tissues after various remediations with free DOX, PPID without laser and PPID with laser lighting are revealed in Fig. 6. Few tumor cells died after 24 h remediation with free DOX (IC_{50} = 1.3 μg/mL), a greater number of the cells significantly died with PPID NPs (IC_{50} = 0.72 μg/mL) and these cells were approximately completely died after laser illumination (IC_{50} = 0.22 μg/mL) meaning that PPID NPs possibly will merge PTT/PDT and chemotherapy to apply synergistic effects in cancer tissues.

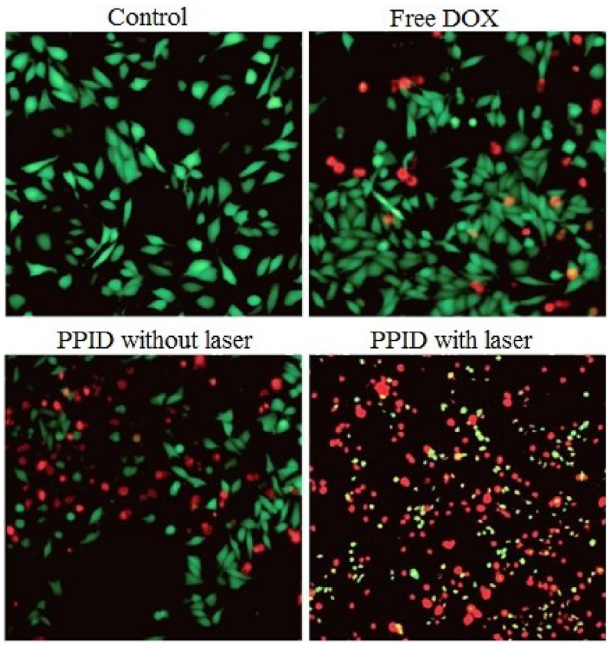

Figure 6 Fluorescence microscopic photographs of live and dead Hep1-6 tissues after various treatments. Reprinted with permission from Ref. 177. Copyright@2019 The Royal Society of Chemistry. Scale bar: 200 μm.

4.2.2. *o-Nitroaryl thioketal carriers*

In an interesting study, Men et al.[178] have presented a new cleavable polymer containing *o*-nitroaryl thioacetal structure with more stability than reported thioketal and thioacetal-based polymers to ROS. They first used *o*-nitrobenzaldehyde (*o*-NBA) and a dithiol derivative for the preparation of thioacetal polymer containing thiol terminated polyTNB. It can be easily conjugated to methoxypolyethylene glycol maleimide (*m*PEG-maleimide) through *m*PEG-maleimide click chemistry. The prepared amphiphilic polymers PEG-polyTNB capable of forming NPs in a combination of THF/dioxane with Nile Red as a hydrophobic drug pattern have been utilized as a light-cleavable nano-drug assembly (Scheme 10). The treatment of PEG-polyTNB with some ROS types specified a significant shift in the oxidation potential of these thioacetal compounds due to the presence of EWD group (NO_2) of NBA, demonstrating improved stability of the polymer against ROS condition compared to the often-reported thioacetal polymers. In addition, irradiation of PEG-polyTNB with UV-A (365 nm) led to ONB product **59** that is subsequently reduced to benzisoxazole derivative **62** and lastly the thioester amine derivative **64** produced, see Scheme 10. Indeed, light leads to degradation of PEG-PolyTNB NPs surface and induced liberation of the Nile red as a hydrophobic drug pattern.

4.2.3. *Metal−organic cage thioketal carriers*

Recently, in a very attractive piece of work, the metal−organic cages (MOCs) were functionalized with ROS-cleavable thioketal linker by Shen et al.[179] (Scheme 11). In this attempt, a ROS-responsive thioketal platform was developed to decrease some dilemmas restrictive biomedical application of MOCs. MOCs are a class of coordination-driven assembly of metallic ions and organic compounds with special hollows that are attractive for DDS[180−188]. The central cavity of MOCs provides new

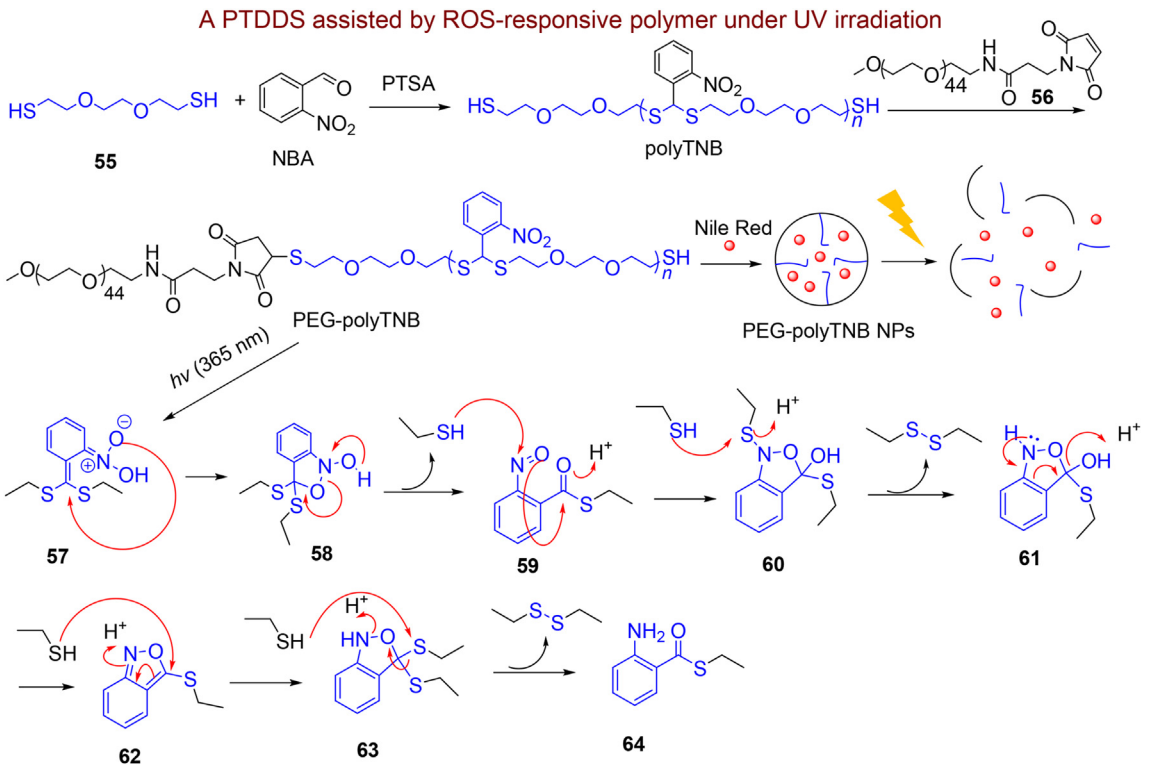

Scheme 10 Synthesis of PEG-polyTNB NPs and its phototriggered release.

opportunities for controlled microenvironments with distinct shape and size that the cavity properties can be modified simply with infinite structural possibilities[189]. This allows that MOCs will be further extended for synergistic result in biomedical fields[190–193]. The ultra-small size of MOCs makes possible tumor penetration; however, the fast release and negligible agglomeration at the cancer cells restrict their biomedical uses[194–199]. As well as, the hydrophobicity of the MOC surfaces progresses internalization on the cancer sites leading to reduced blood circulation period and decreased biocompatibility.

To this end, a ROS-responsive thioketal platform is developed to decrease some dilemmas restrictive biomedical application of MOCs. As described, in this study 3,5-bis(pyridin-4-ylethynyl) aniline (BPA) and PEGylation dithioketal BPA (*m*PEG-SS-BPA) coordinate with Pd^{2+} to form MOCs and then it filled with photosensitizer Zinc Phthalocyanine (ZnPC) in the cavity called ZnPC@polySCage. Heteroleptic strategies were utilized to synthesis of ZnPC@polySCage and construct a cantellated tetrahedral cage using Pd(II) ions and two bent dipyridyl ligands[200–202]. The prepared ZnPC@polySCage can easily penetrate in the depth of cancer cell due to its nanoscale particle size (less than 10 nm). Then, the cavity-loaded ZnPC provided ROS for the degradation of PEG thioketal bond and PDT to destroy the cancer tissues. Interestingly, the PEG dissociation caused surface switching from hydrophilic to hydrophobic and automatically and simultaneous accumulation of MOCs (sizes as big as 671 nm). Therefore, the cellular uptake, tumor accumulation and the PDT efficacy were significantly enhanced under subsequent laser irradiation in the tumor cell. As illustrated in Fig. 7a. The mice mediated with ZnPC@polySCage upon exposure to light compared to only irradiation, ZnPC@polySCage without irradiation, ZnPC with irradiation, and ZnPC@polyCage with irradiation exhibited the significant anti-tumor effect that showed the phototriggered cellular sorption, drug aggregation and the PDT efficacy. Also by comparison, the *in vivo* safety evaluation results revealed that ZnPC@polySCage can be a prospective structure for tumor treatment with attractive biocompatibility and security. The main difference between ZnPC@polySCage and ZnPC@polyCage is that ZnPC@polyCage does not have thioketal linker in its structure that caused by the reaction of 1,3-bis(pyridin-4-ylethynyl) benzene (BPB), PEGylation BPA (*m*PEG-BPA) as well as Pd^{2+} and then filled with ZnPC according to Fig. 7b. The ZnPC@polyCage showed weaker tumor activity compared with ZnPC@polySCage due to diminished aggregation of ZnPC loaded in MOCs.

4.3. *Maleimide-anthracene linker*

Maleimide-anthracene linkers with excellent thermal stability (up to 200 °C) have been utilized as mechanophores to explore the effects of macromolecular architecture or micellar aggregation on the duration of cycloreversion[203–208]. Mechanophores, a class of stimuli-responsive compounds, have recently fascinated the interest of engineers due to their prospective applications as stress sensors[209–213]. These mechanically responsive molecules undergo fluorescent/color changes by the imposition of a mechanical stimulus such as stretch or rotation[214–217]. More recently, Kabb et al.[203] designed a crosslinker rely on the maleimide-anthracene linkage and employed in preparing exclusive networks that exhibit a fluorescence response when damaged by compressive forces. From a mechanistic point of view, the cycloreversion of adduct occurs through pressure and release of the fluorescent anthracene groups as shown in the top inset of Scheme 12. Accordingly, Cheng et al.[218] recently synthesized ultra-stimuli responsive systems based on multiarmed poly(ethylene glycol)-block-poly(ε-caprolactone) (PEG-*b*-PCL) copolymer-linked by

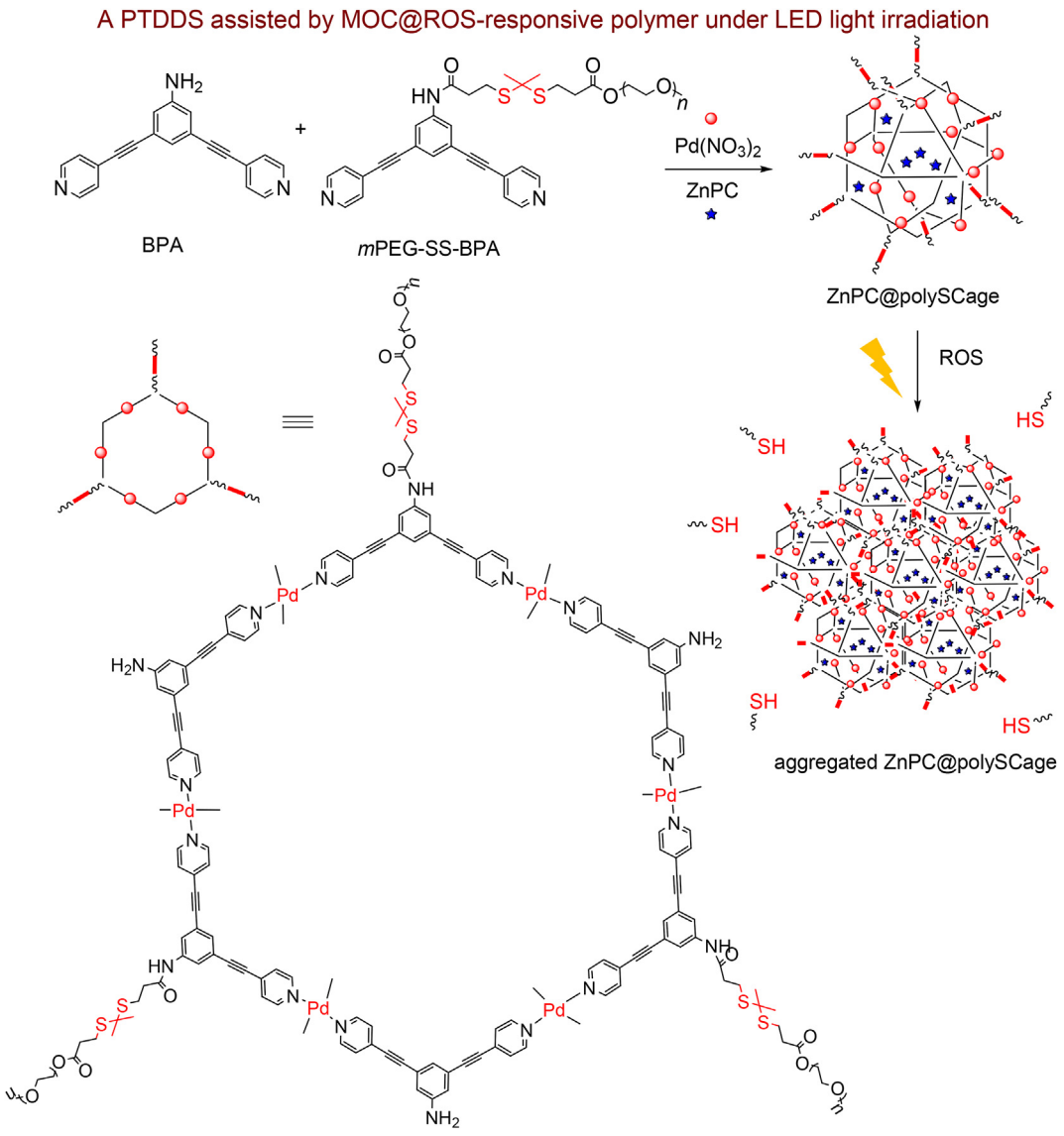

Scheme 11 Synthesis of ZnPC@polySCage and related photoinduced ROS-cleavable pathway.

maleimide-anthracene as a photoresponsive segment to organize a globular phototriggered micellar NPs (maleimide-anthracene@-PEG-*b*-PCL) in aqueous and phosphate buffered saline solution for the controlled drug release (Scheme 12).

A part from various advantages like biodegradability and biocompatibility for clinical usages, the application of PEG-*b*-PCL polymeric micelles as DDS still is limited by the poor hydrolytic dissociation of the PCL segment in the aqueous surroundings. To overcome this obstacle a maleimide-anthracene linker as an ultra light-sensitive group was attached to the PEG-*b*-PCL polymers to generate micelles with unique responsiveness and amphiphilic characteristics. The including of the three PEG fragments in the copolymer structures significantly enhanced hydrophilicity and cause to the development of self-assembled hierarchical arrangements in water with DOX as a hydrophobic drug. As shown in Scheme 12, when DOX-loaded micelles irradiated with UV light (254 nm) for 10 s, the maleimide-anthracene linker disrupted, segments of **65**, **66** produced and the drug rapidly and completely released from micellar NPs. These micellar NPs exhibited a small critical micellar concentration (below 10^{-5} mg/mL), potential micellar stability, improved-controlled photoresponsive property, appropriate drug-loading and ultra-sensitive light-responsive drug-release performance (for only 10 s) and could develop the protection and efficiency of chemotherapy.

4.4. *Photochromic derivatives*

In recent years, photochromic compounds integrated into the supramolecular systems have been extensively applied in phototriggers-based DDSs[137,219–227]. To date, a variety of photochromic derivatives such as stilbene[228–230], spiropyranes[231–235], spirooxazine[236,237], dithienylethene[238–241], azobenzenes[242–246] and 1,3-diazabicyclo[3.1.0]hex-3-ens, as a rather less renowned photochromic derivative[247–251] have been developed that undergo structural changes through rotation or inversion on the original double bond, ring-opening process or the mixture of both processes in response to light irradiation. PTDDSs can be either reversible or irreversible depending on the type of the substrates that absorb the light. PTDDSs containing non-

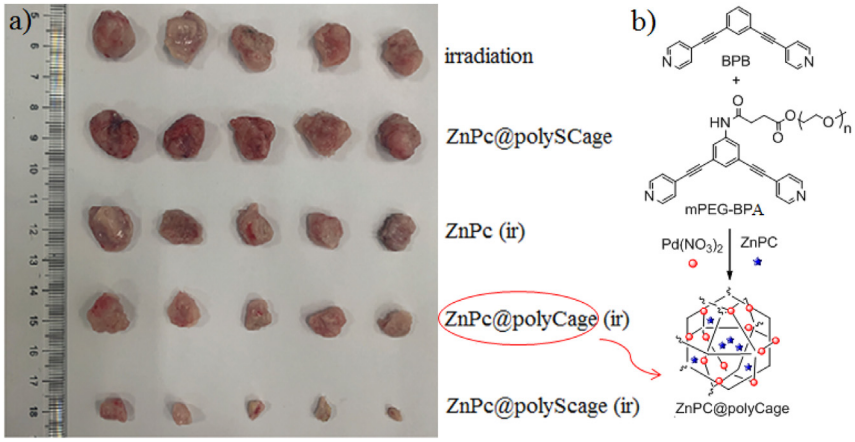

Figure 7 (a) The photographs of the cancer tissues after the mice were sacrificed and (b) synthesis of ZnPC@polyCage. Reprinted with permission from Ref. 179. Copyright@2021 John Wiley & Sons, Inc.

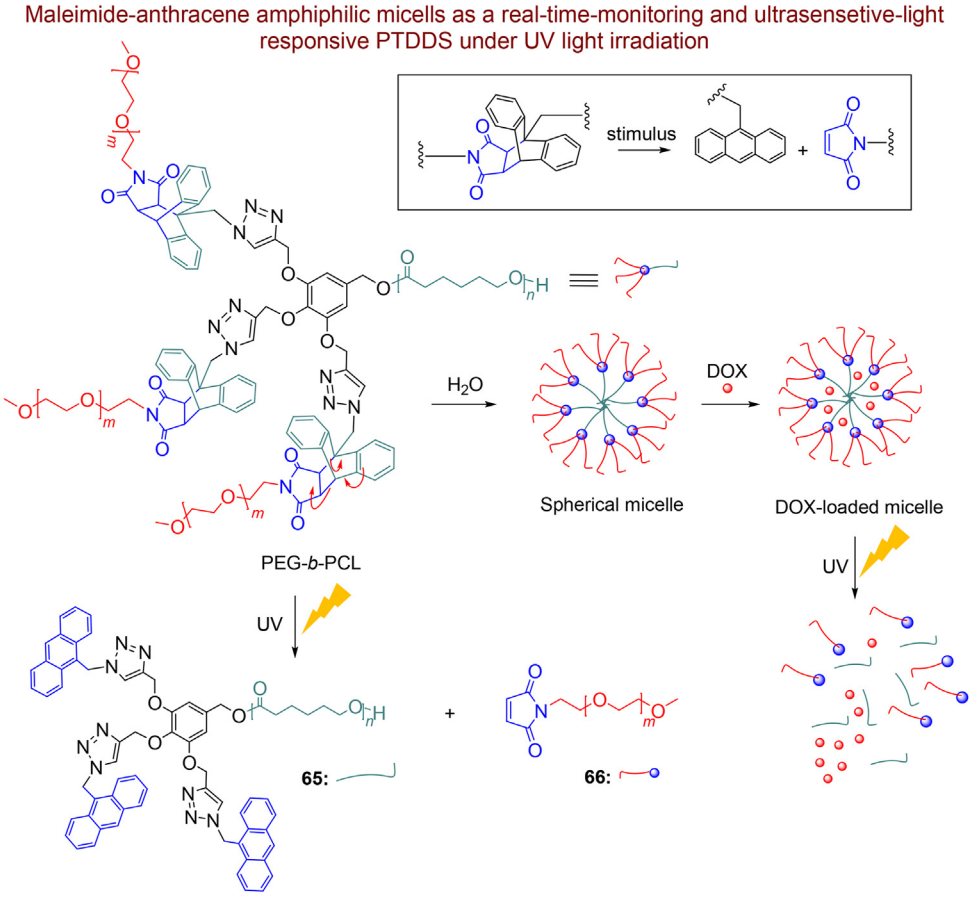

Scheme 12 Structure of maleimide-anthracene@PEG-*b*-PCL micelles, controlled drug loading and phototriggered drug release.

photochromic moiety such as ONB or coumarins mostly undergo an irreversible reaction, whereas PTDDSs based on photochromic molecules show reversible reactions and disordered substrate can be recovered again after removing the applied light. In addition, different light wavelengths can be used to induce light responsiveness. These items show the importance and benefits of utilizing photochromic derivatives in PTDDSs. Lately, almost all PTDDSs based on photochromic molecules are functionalized with photochromic spiropyranes (SP) or azobenzenes (Azo) that can isomerize under UV light irradiation and change their hydrophobic-hydrophilic balance.

4.4.1. Spiropyranes (SP)

SP, as a family of photochromic molecular switches has so far gained particular attention in different DDSs due to inherent biocompatibility and their multi responsiveness to endo-/exogenous

stimuli[60,252–257]. SP undergoes a trigger-induced reversible conversion between the non-planer, hydrophobic and bleached spiro (SP) structure, likewise, the planer, hydrophilic, zwitterionic and colored merocyanine (MC) structure by the breaking of the C_{spiro}–O bond[258,259]. These conversions are highly sensitive to environmental conditions including surface or solvent polarity, pH, ionic strength dependence, hydrogen bonding and polar–polar interfaces. Therefore, when this molecule was incorporated into the polymers after switching they are able to stimulate a considerable alteration in the polymer properties like polymer hydrophobicity[219,260,261]. The majority of phototriggered DDSs expressed here are founded on induced disruption and disorder of the drug carriers that experience an untimely release before arrival at the desired site. In addition, due to the non-reversibility and probable toxicity of the residual carrier pieces it can be appropriate to enable reversible photo-induced DDSs. They work through the intermolecular interplay (work of adhesion) among polymer, drug and solvent without the disruption of the carrier and according to desorption or release of the drugs[262–264]. In an exciting work, Ghani et al.[265] established a photo-responsive interpenetrating polymer networks (IPN) as a new PTDDS, for the first time by the notion of work of adhesion. The work of adhesion declares when, the hydrophobic SP unit in the polymer converts to the hydrophilic MC, the phototriggered drug release can be done without decay and disconnection of the PTDDS. Therefore, the release (desorption) and adsorption of the drug can be frequently changed on and off, only by changing the light on and off. In this study, supercritical carbon dioxide ($scCO_2$) tools were employed to produce IPNs using saturating silicone elastomers (as the host polymer) and copolymers of the photochromic spiropyran methacrylate (SPMA) as the guest polymer with varying hydrophilicity. Overall, the guest polymer mixture, particularly the hydrophilicity of the guest polymer, was the main point in the work of adhesion, untimely and triggered releases. The triggered-release of five different drugs doxycycline hyclate, dopamine, levodopa, prednisone and curcumin with varying hydrophobicity was evaluated, as illustrated in Scheme 13. After illumination of IPNs upon 365 nm UV light, conversion of the monoecious hydrophobic spiropyran to the hydrophilic zwitterionic merocyanine resulted due to a C–O bond division. As a consequence, the release of the drug was done as a result of the intermolecular interplays among the drug, the guest polymer and the solvent without the disruption of the system. Further, for the first time the release of drug can be increased or halted upon illumination in the form of reversible.

4.4.2. *Azobenzenes (Azo)*

Azo derivatives are excellent molecular switches that show great potential application in DDSs because they can be spontaneously, efficiently and reversibly switched between linear trans and bent *cis* forms under UV–visible light illumination[266–273]. This transformation generates the supramolecular azo components reversible self-assembly and dissociation during light irradiation (UV and visible)[274–281]. Also, using hydrophobic interplays and intermolecular van der Waals interactions, *trans*-Azo with an almost flat structure can spontaneously penetrate to the host molecules hollow and undertake complexation, while *cis*-Azo is unable to perform this due to the size difference between the host and guest structure[282–295]. So, *cis*-Azo as a dynamic component and *trans*-Azo as a passive component are candidates for DDS and controlled arrangements[268,296–299]. Wang et al.[300] have prepared and studied a new *in vivo* DDS with hypoxic-responsive Azo bridge *via* efficient reduction of Azo segment to aniline groups using reductases and their surroundings oxygen deficiency, causing in the hypoxia-triggered drug release and giving a synergistic chemotherapy drug DOX with PDT on the inhibition of cancer progress. In other research, Bian et al.[301] designed a photo-responsive silicone in accordance with host-guest interplays between thiolated Azo and β-cyclodextrin (β-CD) intended for controlled cell adhesion of particular cells (MCF-7). The selected tumor cell capture, particular aptamer (Section 2.2, a 25 mer DNA aptamer as GCA GTT GAT CCT TTG GAT ACC CTG G), was attached to the thiol-terminated-azobenzene by chemical coupling reactions for smart capture of MCF-7 when incubating a mixture of cells. Upon UV illumination, the Azo isomerized from *trans* to *cis* photoisomer and the *cis*-Azo cannot be known by β-CD thus releasing the captured MCF-7 cells. These innovative results give a novel avenue for the separation and assessment of tumor cell, mainly for regulated drug release. Therefore, Azo derivatives can be suitable for pharmaceutical and biomedical science due to its responsibility to light, hypoxia and enzymes, so showing gaining increasing attention in site-specific smart cargo delivery and prodrug[302–306]. The employment of Azo derivatives for triggered prodrugs and DDSs, and application of photoswitchable azo-based prodrugs, has been previously reviewed[307].

4.4.3. *Dual-stimuli-responsive phototriggers*

4.4.3.1. Dual-stimuli-responsive SP-triggers. In recent years, the development of dual or multiple stimuli-responsive supramolecular DDSs has attracted increasing attention to suggest a safe and more efficient controlled drug release in cancer microenvironments and with better stability in normal cells using the synergistic retort to diverse triggers and thus reduce the hurt to normal tissues[308–313]. Razavi et al.[314] developed an interesting amphiphilic light/temperature sensitive block copolymers **67** using a hydrophobic poly(methyl methacrylate) (PMMA) segment with

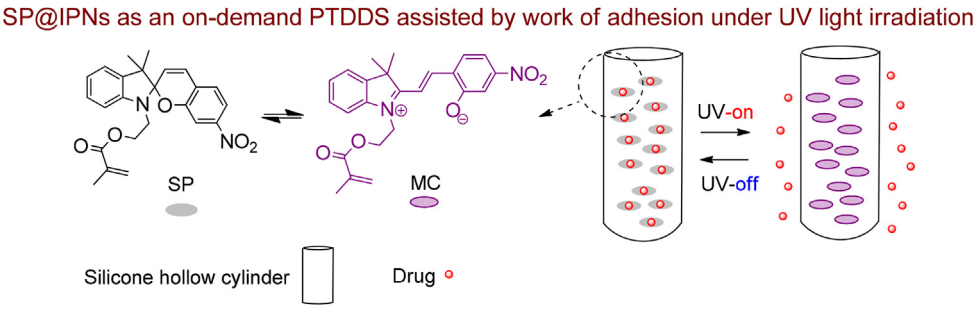

Scheme 13 Desorption and liberation of bioactive components from the photoactive guest polymer in an IPN.

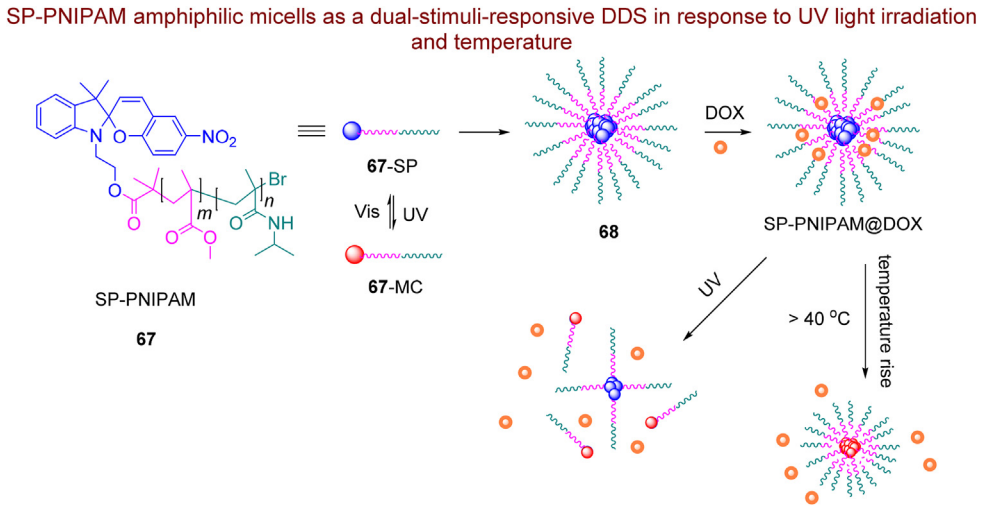

Scheme 14 Self-assembly of SP-PNIPAM of and controlled release of DOX in different conditions.

spiropyran unit as a light responsive group (UV and visible light irradiation) and poly (*N*-isopropylacrylamide) (PNIPAM) segment as a temperature-responsive moiety for controlled DOX release (SP-PNIPAM@DOX, Scheme 14). The amphiphilic copolymers can be self-assembled to nanomicelles in acetone and water solution with a hydrophobic core PMMA and the SP units and a hydrophilic PNIPAM shell. Subsequently, the anticancer drug DOX was loaded into the polymer assemblies **68**. When SP→MC isomerization was performed upon exposure to UV light (365 nm), a movement of the polar MC units to the micelles surface, together with shrinkage of the micellar assemblies induced and DOX release triggered from micelles. This process was completely reversible under visible light irradiation. Besides, the shrinkage of the micellar assemblies occurred in response to temperature increase. PNIPAM has a LCST range of 31−33 °C and the PNIPAM's LCST demonstrated light-dependence. Under UV light irradiation, the LCST of PNIPAM enhanced to 37 °C due to the formation of the polar and water-soluble MC form after isomerization. Therefore, a considerable enhance in release of DOX was done under UV light irradiation and at temperatures over the PNIPAM's LCST (T = 40 °C) in acidic media. These polymer assemblies can be more efficient and applicable for multi-responsive DDSs by light, temperature and pH[315,316].

Further study by the same group, considered a multi-responsive polymer assembly based on SP and poly(-dimethylaminoethyl methacrylate) (PDMAEMA) as a multi-responsive and hydrophobic polymer[317]. The PDMAEMA are generally used as a multi-responsive block toward different stimulants like temperature, pH and CO_2 gas[318−321]. In this study, dynamic light scattering (DLS) consequences indicated that the dimension of polymeric assemblies altered in response to light irradiation, temperature rising (above the LCST of PDMAEMA) and also pH variations (from 5 to 9) accordingly, DOX release was controlled by light irradiation, temperature changes and pH.

4.4.3.2. Dual-stimuli-responsive Azo-triggers. Cheng et al.[322] developed pH/temperature responsive adenine poly(propylene) glycol-functionalized boron nitride nanospheres (BN-APPG) for regulated drug delivery and release in answer to internal pH and temperature stimuli in tumor tissues. While the cancer microenvironment has a somewhat higher temperature and a less pH than the surrounding healthy cells, these nanospheres showed excellent anticancer effect *in vitro*.

To further the development of multiple stimuli responsive DDSs with photo-response performance, Zhang et al.[323] designed and synthesized an interesting dual light/pH-responsive supramolecular polymer *via* the host-guest interaction between β-CD-graft-poly(2-(dimethylamino)ethyl methacrylate) (β-CD-*g*-PDMAEMA) and Azo substituted poly(ε-caprolactone) (Azo-PCL) (Scheme 15). The supramolecular polymer β-CD-*g*-PDMAEMA@Azo-PCL can encapsulate DOX as spherical drug-loaded micelles and exhibits dual stimuli response to changes in light and pH. The hydrophobic PCL linkage as supramolecular micelles core is sensitive to light irradiation and the hydrophilic PDMAEMA moiety utilized as the micelle shell for response to pH changes. According to Scheme 15, Azo with *trans*-configuration can penetrate to the β-CD hallow during the host-guest complexation upon visible light irradiation. After UV illumination, the Azo configuration changes from the trans to *cis*, which cannot be recognized by the β-CD molecules. Therefore, the supramolecular micelles interrupt, causing the release of the DOX drug. Alternatively, in the acidic pH, the completely protonated tertiary amine groups in PDMAEMA moieties develop intense electrostatic repulsion interactions, so accelerating the drug release from the supramolecular micelles[324].

In addition, the electrostatic repulsion, accompanied by low protonation of Azo moieties triggers better inconstancy on the hydrophobic hallow and Azo-PCL core, therefore the host-guest complexation based on β-CD/Azo was weakened and DOX release from micelles was accelerated[324]. Also, under acidic medium, the re-protonation of the DOX amino functional groups enhances the DOX solubility in aqueous media and the micelle cores decay sooner, ensuing in the fast DOX release[325]. UV light irradiation in acidic surroundings more enhances the DOX release than a single stimulus due to synergistic effects of pH and UV light irradiation. These behaviors offer the possibility for the dual DOX-targeted and DOX-controlled release based on diverse physiological situations.

Gao et al.[326] synthesized a dual light/temperature responsive supramolecular polymer brush through the host-guest complexation between β-CD structure on star-like side sequences and

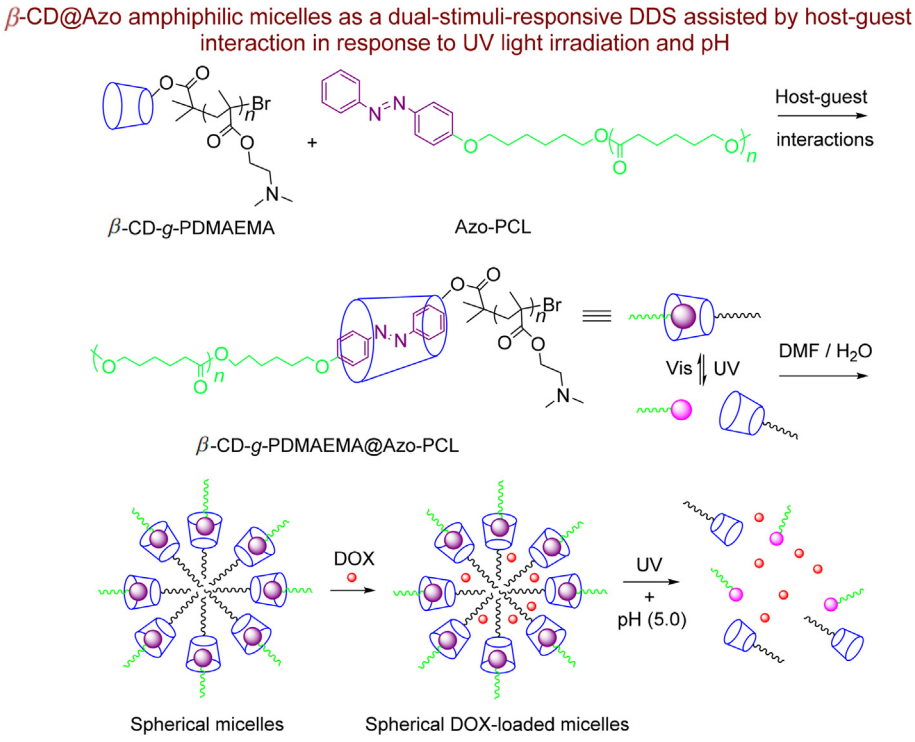

Scheme 15 Preparation, self-assembly and drug loaded of β-CD-*g*-PDMAEMA@Azo-PCL.

Azo moiety as a flexible spine, which supplies a novel platform for the preparation of self-assemblies with special sizes from unimolecular micelles, multi-molecular micelles and vesicles in water *via* alternating UV light irradiation and increasing temperature (Scheme 16). Polymer brushes are a unique kind of joined copolymers that are consists of a pliable unit and interlocked side chains[327–336]. Upon UV light irradiation, the micelles or vesicles are disconnected due to the β-CD is divorced from the Azo backbone during photo-triggered isomerization from *trans* to *cis* conformer. Subsequently, the convened micelles or vesicles are able to accumulate into strawberry superframes *via* rising temperature. This report could be eventuality applied in DDSs.

In the interesting work, Xiao et al.[337] developed a dual stimuli-responsive azo-trigger to independent controlled release of multiple drugs. Since matrix metalloproteinases (MMPs)

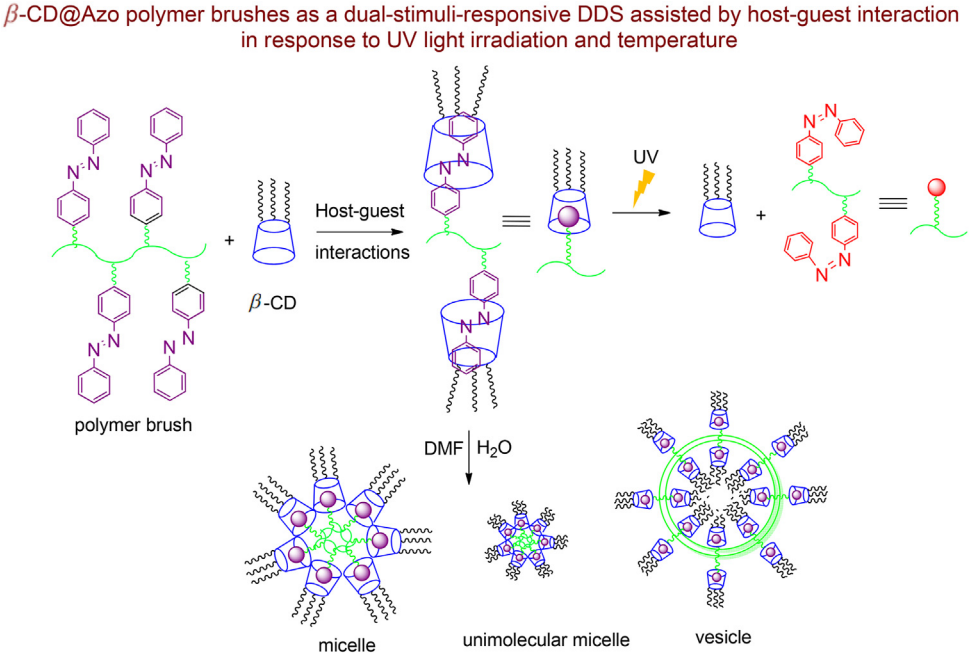

Scheme 16 Self-assemblies of unimolecular, multi-molecular micelles and vesicles through the host-guest interaction.

concentration is overexpressed in cancer tissues, they utilized it as interior stimulus for the controlled release of macromolecular drugs. UV light also used as secondary external stimulus for release of small molecule drugs. According to Scheme 17, the nanospheres were assembled by five bilayers of two particular polymer chains containing poly(acrylic acid-graft-azo-graft-proline-leucine-glycine-valine arginine-adamantane) (PAA-*g*-azo-*g*-PLGVR-AD) and poly(asparticacid-graft-*β*-CD) (PASP-*g*-*β*-CD) *via* layer-by-layer (LbL) method. The PASP-*g*-*β*-CD prepared by the ring-opening reaction of poly(L-succinimide) **81** with mono(6-(2-aminoethyl) amino-6-deoxy)-*β*-cyclodextrin **80** that functionalized firstly by *p*-toluenesulfonyl chloride and then ethylenediamine. The hydrophobic cavities of PASP-*g*-*β*-CD supplies possibilities to load guest molecules *via* non-covalent interactions. Also, the click reaction of alkynyl-terminated **76** with an adamantly azide derivative of **77** afford the PAA-*g*-azo-*g*-PLGVR-AD polymer. The azo-alkynyl-terminated **76** was prepared by cautiously controlling the reaction between conditions from both **69** to **71** and **73** to **76**. This system can load two different drugs, macromolecular drugs were adsorbed in the hollow central cavity of nanospheres while, small molecule drugs attached by *α*-CD that aggregated on layers during the host−guest interaction between *α*-CD and Azo moiety. In this system, dextran$_{5000}$-fluorescein isothiocyanate (Dex$_{5000}$-FITC, with green fluorescence color) as a macromolecular model drug, *α*-CD-rhodamine B (*α*-CD-RhB, with red fluorescence color) as a small molecule model drug, and squamous cell carcinoma (SCC-7 cells) as high MMP activity were chosen. In the tumor tissues connection between AD and *β*-CD can be interrupt because PLGVR peptide hydrolyzed by MMPs and the macromolecular drugs regularly release from cavity. In addition, under UV irradiation, *α*-CD modified small molecule drugs that still bonded to PAA-*g*-azo polymers released from layers during photo-triggered Azo isomerization from trans to cis that this moment, the liberation of the small drugs occurs. The confocal microscopy images of SCC-7 cells confirm that the release of dual drugs can restricted by various stimulation of MMP or UV light irradiation, allowing cocktail treatment for tumor tissues.

5. Dual-releasing phototriggers

Recently, dual-releasing PTDDSs have become a promising approach mainly in biomedical applications over single-releasing phototriggers due of their exceptional properties of quick and clean opening with spatio-temporal manage in the releasing two anticancer drugs and its application in combination treatment[338–343]. Dual-releasing PTDDSs can be released two

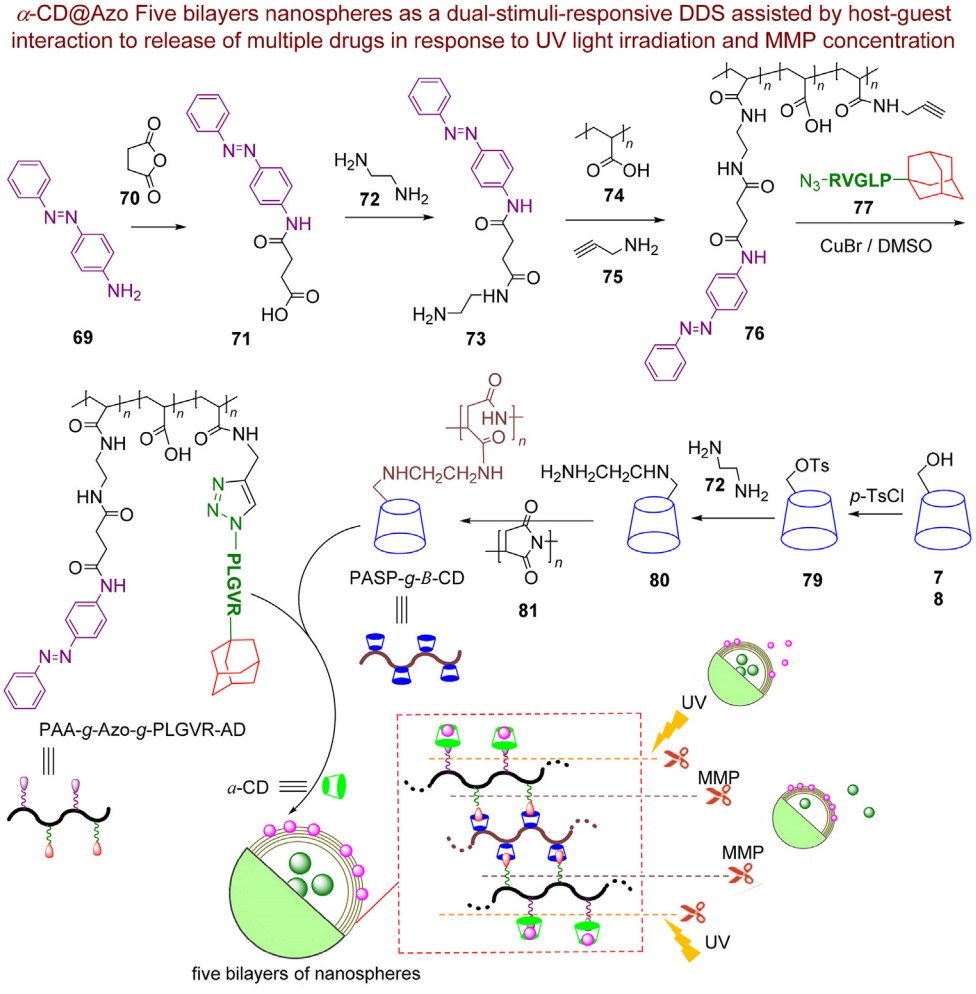

Scheme 17 Synthesis route of five bilayers nanospheres and schematic illustration of drugs release.

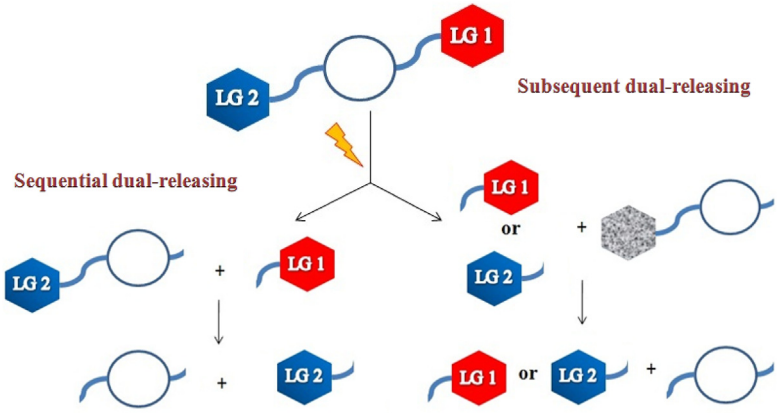

Scheme 18 The schematic illustration of sequential and subsequent dual-releasing phototriggers.

equivalent similar or different active molecules upon exposure to light as sequential (in order) or subsequent (irregular) according to Scheme 18. In the sequential release, the second active molecule is usually in the locked state when the first active molecule release simultaneously during light irradiation. Hence, this approach can exploit for the controlled release of two different active molecules selectively *via* stepwise pathways.

5.1. *Sequential dual-releasing phototriggers*

5.1.1. *Acetyl-nitrobenzyl (ANB) moiety*

Firstly, Bochet et al.[344] established a phototrigger for the sequential release of different LGs by orthogonal photolysis, although, this method requires two- or more-chromophoric structures. Since, the 4-acetyl-2-nitrobenzyl (ANB) segment is able to orthogonal photochemical release of distinct LGs, Kammari et al.[345] synthesized a mono-chromophoric structure **76** during several steps[345]. The mono-chromophoric structure **82** design based on two well-known phototriggered molecules including ANB and phenacyl for the sequential release of two different LG in the presence of a chemical activator and UV light irradiation (<350 nm) (Scheme 19). Upon irradiation, initially, carboxylic acid or alcohol (R−OH) released essentially from ANB segment **82** which its photochemistry is firstly based on a conventional intramolecular 1,5-H shift by the nitro group **82** and formation of aci-nitro intermediate **83**. Subsequently, formation of benzoxazolidines **84** and ring opening occur to release the first LG along with 2-nitrosobenzaldehyde derivative **86**[156,346]. The second LG ($R'CO_2H$) in the phenacyl position of **86** is photochemically released in the presence of a hydrogen atom donor like 2,2-propanol and light if required through photochemical electron transfer[347]. The most important restriction of this study is the necessity of using a chemical activator together with light for the second liberation phase and the sequential manage blocked if the 2,2-propanol (chemical activator) appended at first.

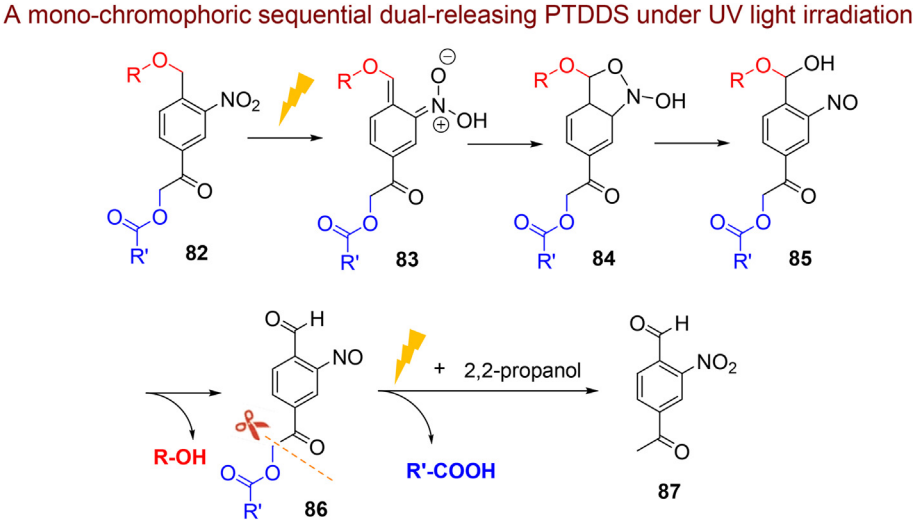

Scheme 19 The structure and photochemistry of phototrigger substituted **82** in the benzylic and the phenacyl positions with LGs.

5.1.2. *o-Hydroxycinnamate*

In a valuable study, Paul et al.[348] proposed a new approach for the sequential and *in situ* release of second active molecule from mono-chromophoric phototrigger **88** no need for an activator (Scheme 20). The first release (alcohol derivatives) occurs from *o*-hydroxycinnamate **88** as phototrigger I, due to the photo-isomerisation of the double bond afterward lactonization during UV light irradiation. The second release (carboxylic acid derivatives) take places *in situ* simply from the generated coumarin **89** as second phototrigger, this step is located in an inactivated state throughout the first deprotecting step. The intended system also has real time monitoring capabilities owing to generation of fluorescence coumarin derivatives.

5.1.3. *Metallopolymer*

He et al.[349] developed a sequential dual-releasing phototriggered metallopolymer (Poly@Ru/PTX) for release of photosensitizer ruthenium complex (Ru) and paclitaxel (PTX) as an anticancer drug for the first time (Scheme 21). The polymer filament includes methoxy polyethylene glycol (MPEG) and piperidine-functionalized polycarbonate (PTMCP) that Ru complexes and PTX covalently appended to the polymer backbone using a superficial amino-alkynoate click polymerization[350]. This type of innovative connection could let Ru and PTX to attain cancer spots concurrently *via* enhanced permeability and retention (EPR) effects and eschew unwanted drug release in the bloodstream. The red-light irradiation of the cancer cells released the anti-tumor Ru complexes straightforwardly and produced reactive singlet oxygen ($^1O_2$). The released $^1O_2$ can cleave the ROS-sensitive β-amino-acrylate bond during oxidative degradation resulting to the liberation of PTX and other products **91**, **92**. The *in vitro* and *in vivo* investigations of poly(Ru/PTX) confirm a synergistic effects of chemotherapy PTX with PDT with exceptional cancer accumulation, cytotoxic activity (lower 32.4% viability) and high biosafety under red light irradiation.

5.2. *Subsequent dual-releasing phototriggers*

5.2.1. *Carbazole-combined to o-hydroxycinnamate*

Carbazoles are of great importance among nitrogen containing heterocycles mostly due to efficient luminescence property[351], various biological performances[352] and easy modification and functionalization of core frame[353]. Accordingly, Venkatesh et al.[354] designed a carbazole-combined to *o*-hydroxycinnamate derivative **93** for the subsequent dual release of similar and different alcohols upon one- and two-photon excitation (Scheme 22). The mechanism for the dual release upon irradiation progresses through excitation of **93** to its singlet state **94** and then a *trans*−*cis* isomerization leading to the release of first alcohol and arrangement of the newly coumarin carbazole Cou-CBZ. The second LG also release by following a similar mechanism. The first and second release confirmed by an increase in fluorescence intensity and fluorescence color change, respectively. Since, in the Cou-CBZ internal charge transfer (ICT) take places between one carbazole moiety (as donor) and one ester-carbonyl moiety (as an acceptor) the fluorescence intensity is higher than Cou-CBZ-Cou. Furthermore, the fluorescence color change (from green to blue) is because, in Cou-CBZ-Cou, ICT does not occur. Although, the limitation of this work is the coumarin carbazole byproducts can operate as an inner filter.

5.2.2. *Acetyl carbazole*

The same group[355] synthesized a fluorescent dual-releasing phototrigger substrate (CBZ-CA-Cbl) based on acetyl carbazole chromophore with two arms to photocaging and subsequent release of both caffeic acid (CA) and Cbl simultaneously after UV light irradiation. Irradiation of CBZ-CA-Cbl causes to a singlet excited state **96** that undergoes ISC to their triplet state **97** and then cleavage of the C−O bond in carbazole continues **97** to form anion-pair intermediate **98**. Solvation of the ion-pair intermediate **98**, gives hydroxyacetyl **99** and released first drug. The second drug also release by related mechanism. By using the natural product CA, this dual-releasing phototrigger displayed improved anticancer effect (lower 45% viability, IC_{50} at 15 μmol/L) in comparison to single-releasing phototrigger CBZ-Cbl (60% viability) and even CBZ-CA (above 75% viability) (Scheme 23).

5.2.3. *Functionalized acridines*

Acridine derivatives with the planer structure are a DNA intercalator and topoisomerase II inhibitor[356,357] that widely considered for their anticancer and antibacterial properties[358–362]. These results afforded the opportunity to develop acridine-based phototriggers for controlled release of drugs. Zhuang et al.[363] first described C9-functionalized acridine phototrigger for the release of different alcohols under UV light irradiation. Furthermore, Jana et al.[364] and Piloto et al.[365] utilized the same C9-functionalized acridine phototrigger to the liberation of carboxylic acids and neurotransmitter amino acids. However, this phototrigger can liberate just one LG, limiting its application in combination treatment. Ray et al.[366] designed a C4- and C5-functionalized acridine with dual arm to protection and then release of two anticancer drugs Cbl and valproic acid (Vpa) simultaneously

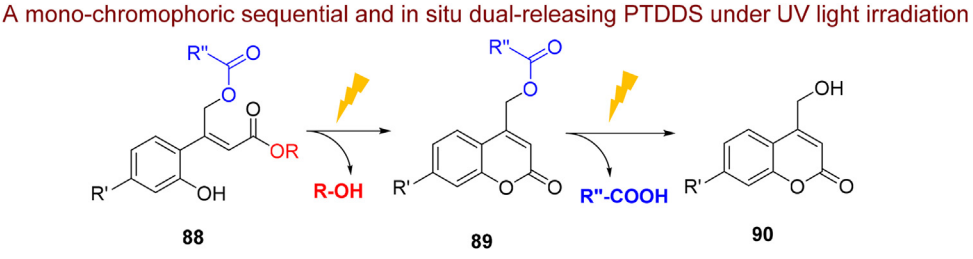

Scheme 20 The structure and *in situ* liberation of phototrigger substituted **88** with different LGs.

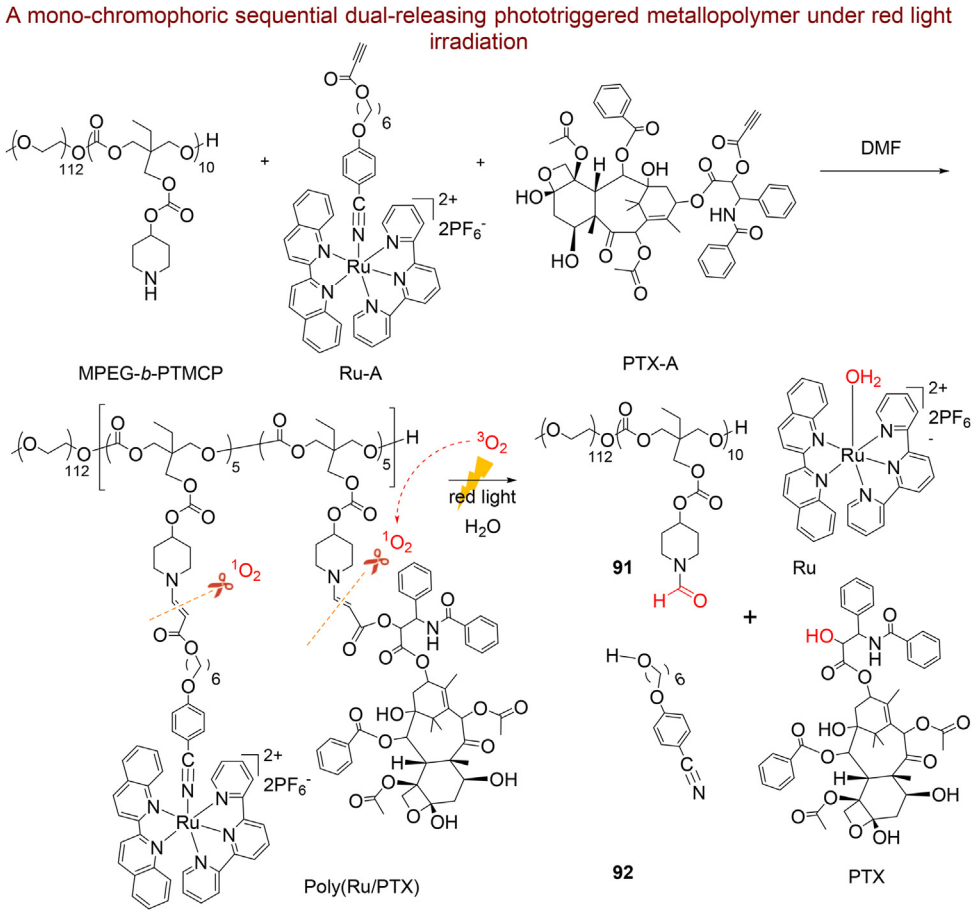

Scheme 21 The synthetic route of poly(Ru/PTX), cleavage of β-aminoacrylate bond and release of drugs and other products **91**, **92** after oxidative degradation.

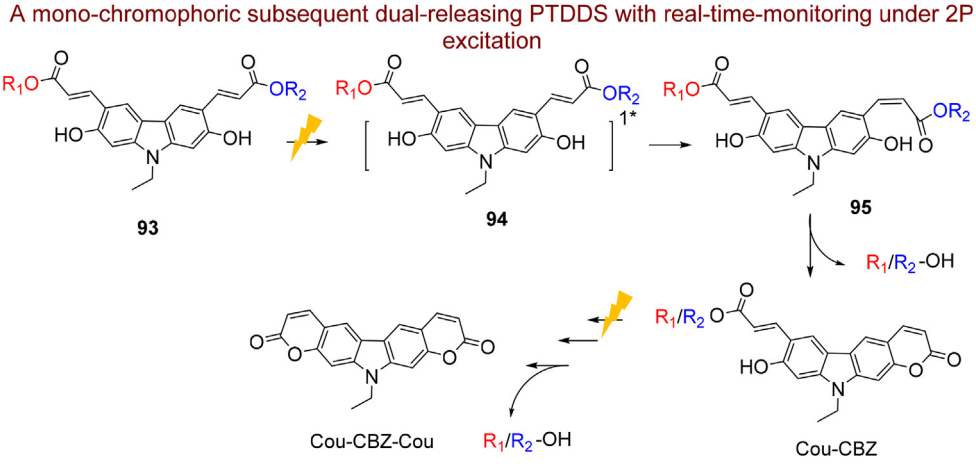

Scheme 22 The structure of dual-releasing phototrigger **93** and subsequent release of alcohols.

under visible light irradiation ($\lambda \geq 410$ nm) (Scheme 24). The photorelease pathway upon visible light irradiation is as follows: firstly, Acr-Cbl-Vpa excited to its singlet state and then undertakes a heterolytic C−O bond dissociation at the C4 or C5 benzyl substituent **101** to yield anion pair **102** that after solvation, one equivalent of Cbl or Vpa liberated. Subsequently, the attained acridine **103** once more excited to its singlet state and generates another equivalent of Cbl or Vpa. Irradiated Acr-Cbl-Vpa-

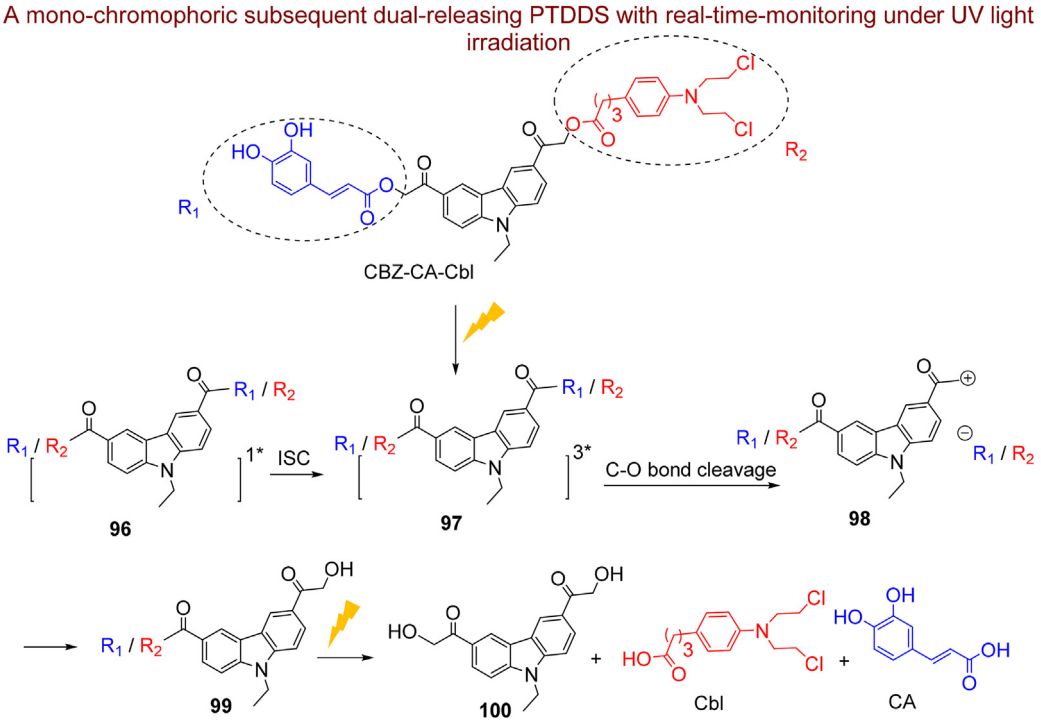

Scheme 23 The CBZ-CA-Cbl structure and subsequent dual-release of CA and Cbl.

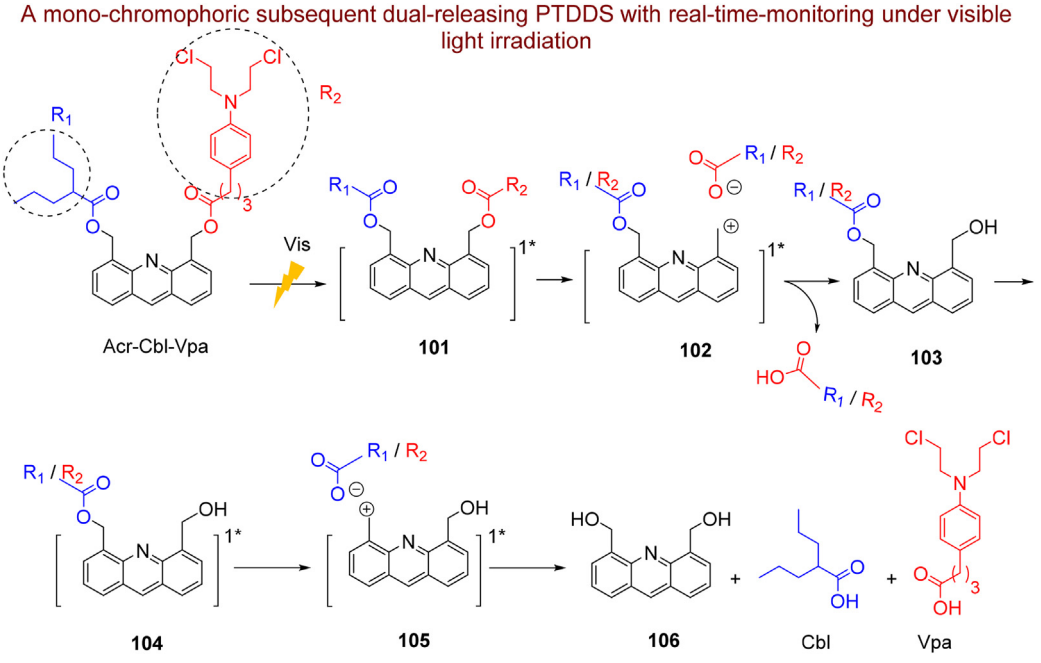

Scheme 24 The Acr-Cbl-Vpa structure and subsequent release of Vpa and Cbl.

incubated cells with visible light showed approximately double cytotoxicity (EC_{50} = 12.59 μmol/L) than free Cbl (EC_{50} = 20.23 μmol/L) with a synergistic efficacy of Vpa upon Cbl. This dual-releasing phototrigger also illustrated the real-time monitoring ability from green (uncleaved nano-drug) to blue (cleaved nano-drug) color change through photolysis.

5.2.4. Salicylaldazine

Biswas et al.[367] have selected salicylaldazine (SDA) as the fundamental chromophore, which displays AIE and ESIPT process simultaneously. As previously mentioned (Section 3.2), the ESIPT incorporated with AIE provide further views to extend PTDDSs to drug photorelease with more efficiency in the aggregated state and

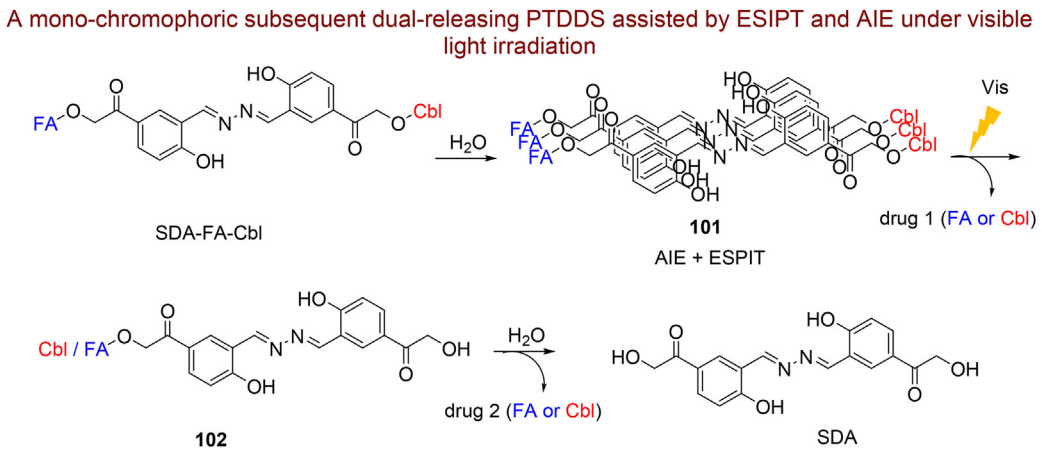

Scheme 25 The structure and photorelease of the dual PTDDS SDA-FA-Cbl.

Table 1 The unique properties of the foresaid PTDDSs in biomedical application.

Entry	PTDDSs	Unique property/ies		Ref.
1	*p*HP-Benz-Cbl	PTDDSs based on photochemical bond cleavage	1. Very fast photorelease of Cbl (15 min) upon visible light with distinct fluorescence discolor	108
2	*p*HP-Naph-Cbl		1. Two-photon absorption in the phototherapeutic window (700 nm) 2. Liberation of Cbl only in their aggregated state under visible light irradiation 3. High real-time monitoring ability (from greenish-yellow to blue)	109
3	TPE-pHP-Cbl		1. Liberation of Cbl only in their aggregated state under visible light irradiation 2. High real-time monitoring ability 3. PDT activity	124
4	TPE(Cbl)$_4$ NPs		1. Release of 4 eq Cbl only in their aggregated state under visible light irradiation 2. High real-time monitoring ability, PDT activity	125
5	HBT@*o*-hydroxycinnamate		1. Rapid and shortest release (60 min) of methyl salicylate 2. Distinct fluorescence color change from orange to blue following photorelease	129
6	Carbazole-coumarin derivatives 23,24		1. The phototrigger activates upon visible light irradiation 2. A synergic effect of phototriggered drug release and photosensitization of the carbazole-coumarin segment	144
7	π-Extended coumarin 26-31		1. A two-photon uncaging sensitivity	145
8	Click-and-release system based on coumarin		1. The phototrigger activates upon the blue visible light 2. An extra level of spatial and temporal control for the release of the caged compounds	146
9	Dex@PP52	PTDDSs based on photoinduced disruption of nanoscale structures	1. The phototrigger activates upon the blue visible light 2. The strong visible light absorption above 500 nm 3. Photo-reactivity in hydrophobic surroundings	159
10	PPID		1. A ROS-responsive drug carrier 2. Synergistic effects of PTT/PDT and chemotherapy treatment	177
11	PEG-polyTNB		1. Resistant to high concentrations of ROS unlike reported thioacetal bonds and preventing non-triggered release	178
12	ZnPC@polySCage		1. Ultra-small size of ZnPC@polySCage 2. Hydrophobic ROS-responsive thioketal MOCs 3. PDT efficacy	179
13	Maleimide-anthracene@PEG-*b*-PCL micelles		1. An ultra light-sensitive characteristics (10 s) 2. A small critical micellar concentration (below 10^{-5} mg/mL) 3. Strong hydrolytic dissociation of the PCL segment in the aqueous surroundings	218
14	IPN		1. The drugs releasing without disruption of the system 2. Increasing or halting of drugs release upon illumination	265

(*continued on next page*)

Table 1 (*continued*)

Entry	PTDDSs	Unique property/ies		Ref.
15	Hypoxic-responsive Azo bridge		1. Synergistic effects of chemotherapy DOX with PDT	300
16	Azo@β-CD		1. Smart capture of MCF-7 cells in a mixture of cells under UV irradiation	301
17	SP-PNIPAM@DOX		1. A more enhance in release of DOX under UV light irradiation and at temperatures	314
18	SP-PDMAEMA@DOX		1. The DOX release by light irradiation, temperature changes and pH	317
19	β-CD-*g*-PDMAEMA@Azo-PCL		1. Dual stimuli response to changes in light and pH 2. The very fast release of DOX due to synergistic effects of pH and UV light irradiation	323
20	Supramolecular polymer brush		1. Dual stimuli response to changes in light and temperature 2. Self-assemblies of unimolecular, multi-molecular micelles and vesicles through the host-guest interaction with special sizes	326
21	Five bilayers nanospheres		1. Dual stimuli response to changes in light and MMP concentration 2. The ability to load two different drugs simultaneously	337
22	Mono-chromophoric structure **82**	Dual-releasing phototriggers	1. Sequential release of two different LG in the presence of a chemical activator and UV light irradiation	345
23	Phototrigger **88**		1. The sequential release of two different LG under UV light irradiation no need for an activator 2. High real-time monitoring ability	348
24	Poly@Ru/PTX		1. The sequential release of two different LG under red light irradiation 2. Synergistic effects of chemotherapy PTX with PDT Ru 3. High biosafety under red light irradiation	349
25	Carbazole-combined to *o*-hydroxycinnamate derivative **93**		1. The subsequent dual release of similar and different LG upon one- and two-photon excitation 2. Confirmation of the first and second release by an increase in fluorescence intensity and fluorescence color change, respectively	354
26	CBZ-CA-Cbl		1. Fluorescent subsequent dual-releasing substrate	355
27	Acr-Cbl-Vpa		1. The sequential release of two different LG under visible light irradiation 2. High real-time monitoring ability	366
28	SDA-FA-Cbl		1. The sequential release of two different LG under visible light irradiation 2. Display AIE and ESIPT process simultaneously 3. High real-time monitoring ability	367

dispelling the nonfluorescent character of the phototriggered molecules such as pHP groups. In this study, as displayed in Scheme 25, salicylaldazine moiety functionalized with two different drugs ferulic acid (FA) and Cbl on both sides (SDA-FA-Cbl) by simple merging of salicylaldazine to *p*HP. By virtue of which, it supplies the fast photorelease of two drugs sequentially inside the cell (5 min) with distinct fluorescent color change (from yellow to blue) using visible light irradiation (>410 nm) which confirmed the high efficiency of this phototriggered DDS.

The photochemical release of drugs from SDA-FA-Cbl initiates with AIE phenomena, ESIPT movement from *p*HP moiety to the imine group and then continues during photo-Favorskii rearrangement by forming the putative spirodiketone intermediate similar to what was expressed in Scheme 1. This PTDDS demonstrated a highest level of cytotoxicity towards HeLa cells (above 90%) upon irradiation compared with free Cbl due to effective biodistribution and the synergistic effect of FA and Cbl.

6. Hazard assessment and clinical studies of PTDDS methods

Despite the great attention on the design and effectiveness of PTDDS, it is important to pay attention to the side effects of this method due to the poor understanding of drug−tissue interactions and material properties[368,369]. In addition, it should be considered that the biomaterials and micro- or nanoparticulate formulations are not necessarily inert. Therefore, before use for clinical trials, several issues such as the assessment of formulation's biocompatibility *via in vitro* and *in vivo* sights, the safety of the all components of the PTDDS, including the drugs to be delivered locally and systemically, and mitigating tissue reaction directly *via* decoration and surface modification of particles with appropriate materials, should be addressed, accurately. In addition, it is still troubles to penetrate internal body parts even with IR. In current research, there are few *in vivo* phototargeted evaluations of PTDDSs, for example, Carling et al.[159], Shen et al.[179], and He et al.[349] investigated the *in vivo*

pharmacokinetic activity of prepared phototriggered structures in mice tissue. However, PDT clinically approved as an effective method to cancer treatment[370], while PTT and PTDDS are still in clinical studies to treat cancer[371].

7. Conclusions and future challenge

Various directions have been successfully extended for triggering the release of chemically or biologically moieties using peripheral stimuli, such as light that is a principally noteworthy stimulus. In this review, we have covered latest phototriggered molecules on DDSs together with their main mechanism for triggered drug release. The unique properties of all the mentioned PTDDSs in this review are given in Table 1. Phototrigered molecules are excellent and versatile tools for the release of various chemicals especially bioactive molecules in living tissue. Although various phototriggers have been developed, there are important challenges to be addressed for sensible demands. One of the major challenges to expand the biomedical applications of phototriggers is to increase the diversity of the phototriggers family. In continuation to our prior work[248–251] and despite this study, there has been an upsurge in interest in our group on design and exploitation of photochromic 1,3-diazabicyclo [3.1.0]hex-3-en derivatives to fulfill the demands for increase the variety of the phototriggers. Recently, we (Shamsipur et al.[247]) found that these photochromic structures are able to bind with charged molecules under sunlight. The capacity of these structures for photo-induced binding with active molecules might bring new opportunities to promote the development of innovative and new phototriggers. Furthermore, this family of photochromic derivatives is an excellent photo-responsive connection by short-term exposure to sunlight that may significantly influences their ability to form safe and ultrasensitive PTDDSs.

The type of light employed is another challenge to be improved for phototriggers. Especially NIR light is still worth of note due to deep penetration and safety. Although, sensitized methodology, multiphoton and UCNPs technologies are good examples of long wavelength with adequate energy to stimulate bond breaking, isomerization or rearrangement responses in triggered drug release, however these successes restricted for phototriggers due to their low efficiency values. Other criteria for the appropriate design of PTDDSs, include the following items:

- Strong absorption of phototriggered molecules at wavelengths above 300 nm.
- Fast responses of phototriggered molecules by a short-term light treatment.
- Enhancement of their water solubility.
- Biocompatibility of photo-produced byproducts.
- The phototriggered intermediates or byproducts should not have absorption spectrum in the range of released bioactive components wavelengths to avoid competitive absorption.

In addition, combination of light into dual/multi stimuli-sensitive DDSs and development of single chromophoric PTDDS with simultaneous release of two drugs can lead to unprecedented and precision control over drug delivery, drug release and therapeutic efficacy. If all these requirements can be considered, the prospect of PTDDSs is very brilliant and we can hope that PTDDSs with avoiding unwanted side effects could be implemented in future studies.

Acknowledgments

The support of this work by the Razi University is gratefully acknowledged.

Author contributions

Mojtaba Shamsipur and Atefeh Ghavidast conceived the idea. Atefeh Ghavidast performed the literature search, wrote the original draft and revised the manuscript. Mojtaba Shamsipur and Afshin Pashabadi edited the manuscript. All authors read and approved the final manuscript.

Conflicts of interest

The authors have no conflicts of interest to declare.

References

1. Wang X, Chen X, Yang Y. Spatiotemporal control of gene expression by a light-switchable transgene system. *Nat Methods* 2012;**9**:266–9.
2. Fang L, Zhao Z, Wang J, Xiao P, Sun X, Ding Y, et al. Light-controllable charge-reversal nanoparticles with polyinosinic-polycytidylic acid for enhancing immunotherapy of triple negative breast cancer. *Acta Pharm Sin B* 2022;**12**:353–63.
3. Yamaguchi S, Chen Y, Nakajima S, Furuta T, Nagamune T. Light-activated gene expression from site-specific caged DNA with a biotinylated photolabile protection group. *Chem Commun* 2010;**46**:2244–6.
4. Pinto MN, Mascharak PK. Light-assisted and remote delivery of carbon monoxide to malignant cells and tissues: photochemotherapy in the spotlight. *J Photochem Photobiol C Photochem Rev* 2020;**42**:100341–58.
5. Gupta S, Ahmad N, Mukhtar H. Involvement of nitric oxide during phthalocyanine (Pc4) photodynamic therapy-mediated apoptosis. *Cancer Res* 1998;**58**:1785–8.
6. Jori G, Spikes JD. Photothermal sensitizers: possible use in tumor therapy. *J Photochem Photobiol B Biol* 1990;**6**:93–101.
7. Li MH, Keller P. Stimuli-responsive polymer vesicles. *Soft Matter* 2009;**5**:927–37.
8. Son S, Shin E, Kim BS. Light-responsive micelles of spiropyran initiated hyperbranched polyglycerol for smart drug delivery. *Biomacromolecules* 2014;**15**:628–34.
9. Jiang J, Qi B, Lepage M, Zhao Y. Polymer micelles stabilization on demand through reversible photo-cross-linking. *Macromolecules* 2007;**40**:790–2.
10. Bao C, Zhu L, Lin Q, Tian H. Building biomedical materials using photochemical bond cleavage. *Adv Mater* 2015;**27**:1647–709.
11. Lin FC, Xie Y, Deng T, Zink JI. Magnetism, ultrasound, and light-stimulated mesoporous silica nanocarriers for theranostics and beyond. *J Am Chem Soc* 2021;**143**:6025–36.
12. Karimi M, Zangabad PS, Baghaee-Ravari S, Ghazadeh M, Mirshekari H, Hamblin MR. Smart nanostructures for cargo delivery: uncaging and activating by light. *J Am Chem Soc* 2017;**139**:4584610.
13. Klajn R. Spiropyran-based dynamic materials. *Chem Soc Rev* 2014;**43**:148–84.
14. Requena JM. *Stress response in microbiology*. Norfolk: Calster academic press; 2012.
15. Stevens M, Merilaita S. Animal camouflage: current issues and new perspectives. *Philos Trans R Soc London, Ser A B* 2009;**364**:423–7.
16. Aizenberg J, Tkachenko A, Weiner S, Addadi L, Hendler G. Calcitic microlenses as part of the photoreceptor system in brittlestars. *Nature* 2001;**412**:819–22.

17. Gu H, Mu S, Qiu G, Liu X, Zhang L, Yuan Y, et al. Redox-stimuli-responsive drug delivery systems with supramolecular ferrocenyl-containing polymers for controlled release. *Coord Chem Rev* 2018;**364**:51−85.
18. Malachowski K, Breger J, Kwag HR, Wang MO, Fisher JP, Selaru FM, et al. Stimuli-responsive theragrippers for chemo-mechanical controlled release. *Angew Chem Int Ed* 2014;**53**:8045−9.
19. Rwei AY, Lee JJ, Zhan C, Liu Q, Ok MT, Shankarappa SA, et al. Repeatable and adjustable on-demand sciatic nerve block with phototriggerable liposomes. *Proc Natl Acad Sci U S A* 2015;**112**:15719−24.
20. Luo D, Li N, Carter KA, Lin C, Geng J, Shao S, et al. Rapid light-triggered drug release in liposomes containing small amounts of unsaturated and porphyrin-phospholipids. *Small* 2016;**12**:3039−47.
21. Bagheri A, Arandiyan H, Boyer C, Lim M. Lanthanide-doped upconversion nanoparticles: emerging intelligent light-activated drug delivery systems. *Adv Sci* 2016;**3**:1500437−50.
22. Mura S, Nicolas J, Couvreur P. Stimuli-responsive nanocarriers for drug delivery. *Nat Mater* 2013;**12**:991−1003.
23. Allen TM, Cullis PR. Drug delivery systems: entering the mainstream. *Science* 2004;**303**:1818−22.
24. Sun Q, Wang Z, Liu B, He F, Gai S, Yang P, et al. Recent advances on endogenous/exogenous stimuli-triggered nanoplatforms for enhanced chemodynamic therapy. *Coord Chem Rev* 2022;**451**:214267.
25. Karimi M, Ghasemi A, Sahandi Zangabad P, Rahighi R, Moosavi Basri SM, Mirshekari H, et al. Smart micro/nanoparticles in stimulus-responsive drug/gene delivery systems. *Chem Soc Rev* 2016;**45**:1457−501.
26. Alvarez-Lorenzo C, Concheiro A. Smart drug delivery systems: from fundamentals to the clinic. *Chem Commun* 2014;**50**:7743−65.
27. Timko BP, Dvir T, Kohane DS. Remotely triggerable drug delivery systems. *Adv Mater* 2010;**22**:4925−43.
28. Abbas M, Zou Q, Li S, Yan X. Self-assembled peptide- and protein-based nanomaterials for antitumor photodynamic and photothermal therapy. *Adv Mater* 2017;**29**:1605021−36.
29. Bouchaala R, Anton N, Anton H, Vandamme T, Vermot J, Smail D, et al. Light-triggered release from dye-loaded fluorescent lipid nanocarriers *in vitro* and *in vivo*. *Colloids Surf, B* 2017;**156**:414−21.
30. Lan G, Ni K, Lin W. Nanoscale metal-organic frameworks for phototherapy of cancer. *Coord Chem Rev* 2019;**379**:65−81.
31. Son J, Yi G, Yoo J, Park C, Koo H, Choi HS. Light-responsive nanomedicine for biophotonic imaging and targeted therapy. *Adv Drug Deliv Rev* 2019;**138**:133−47.
32. Liu B, Li C, Yang P, Hou Z, Lin J. 808-nm-Light-excited lanthanide-doped nanoparticles: rational design, luminescence control and theranostic applications. *Adv Mater* 2017;**29**:1605434−57.
33. Shabahang S, Kim S, Yun SH. Light-guiding biomaterials for biomedical applications. *Adv Funct Mater* 2018;**28**:1706635−51.
34. Xu L, Mou F, Gong H, Luo M, Guan J. Light-driven micro/-nanomotors: from fundamentals to applications. *Chem Soc Rev* 2017;**46**:6905−26.
35. Tao Y, Chan HF, Shi B, Li M, Leong KW. Light: a magical tool for controlled drug delivery. *Adv Funct Mater* 2020;**30**:2005029−66.
36. Croissant J, Zink JI. Nanovalve-controlled cargo release activated by plasmonic heating. *J Am Chem Soc* 2012;**134**:7628−31.
37. Liu S, Han MY. Silica-coated metal nanoparticles. *Chem Asian J* 2010;**5**:36−45.
38. Li H, Tan LL, Jia P, Li QL, Sun YL, Zhang J, et al. Near-infrared light-responsive supramolecular nanovalve based on mesoporous silica-coated gold nanorods. *Chem Sci* 2014;**5**:2804−8.
39. Rosensweig RE. Heating magnetic fluid with alternating magnetic field. *J Magn Magn Mater* 2002;**252**:370−4.
40. Lin F, Zink I. Probing the local nanoscale heating mechanism of a magnetic core in mesoporous silica drug-delivery nanoparticles using fluorescence depolarization. *J Am Chem Soc* 2020;**142**:5212−20.
41. Liu X, Zhang Y, Wang Y, Zhu W, Li G, Ma X, et al. Comprehensive understanding of magnetic hyperthermia for improving antitumor therapeutic efficacy. *Theranostics* 2020;**10**:3793−815.
42. Thomas CR, Ferris DP, Lee JH, Choi E, Cho MH, Kim ES, et al. Noninvasive remote-controlled release of drug molecules *in vitro* using magnetic actuation of mechanized nanoparticles. *J Am Chem Soc* 2010;**132**:10623−5.
43. Boissenot T, Bordat A, Fattal E, Tsapis N. Ultrasound-triggered drug delivery for cancer treatment using drug delivery systems: from theoretical considerations to practical applications. *J Contr Release* 2016;**241**:144−63.
44. Lee SF, Zhu XM, Wang YXJ, Xuan SH, You Q, Chan WH, et al. Ultrasound, pH, and magnetically responsive crown-ether-coatedcore/shell nanoparticlesas drug encapsulation and release systems. *ACS Appl Mater Interfaces* 2013;**5**:1566−74.
45. Santini JT, Cima MJ, Langer R. A controlled-release microchip. *Nature* 1999;**397**:335−8.
46. Ni K, Luo T, Nash GT, Lin W. Nanoscale metal-organic frameworks for cancer immunotherapy. *Acc Chem Res* 2020;**15**:1739−48.
47. Yang G, Liu J, Wu Y, Feng L, Liu Z. Near-infrared-light responsive nanoscale drug delivery systems for cancer treatment. *Coord Chem Rev* 2016;**320**−**321**:100−17.
48. Cheng HB, Cui Y, Wang R, Kwon N, Yoon J. The development of light-responsive, organic dye based, supramolecular nanosystems for enhanced anticancer therapy. *Coord Chem Rev* 2019;**392**:237−54.
49. Samadian H, Maleki H, Allahyari Z, Jaymand M. Natural polymers-based light-induced hydrogels: promising biomaterials for biomedical applications. *Coord Chem Rev* 2020;**420**:213432−61.
50. Marturano V, Kozlowska J, Bajek A, Giamberini M, Ambrogi V, Cerruti P, et al. Photo-triggered capsules based on lanthanide-doped upconverting nanoparticles for medical applications. *Coord Chem Rev* 2019;**398**:213013−6.
51. Thang DC, Wang Z, Lu X, Xing B. Precise cell behaviors manipulation through light-responsive nano-regulators: recent advance and perspective. *Theranostics* 2019;**9**:3308−40.
52. Ansari AA, Parchur AK, Chen G. Surface modified lanthanide upconversion nanoparticles for drug delivery, cellular uptake mechanism, and current challenges in NIR-driven therapies. *Coord Chem Rev* 2022;**457**:21442.
53. Yan C, Zhang Y, Guo Z. Recent progress on molecularly near-infrared fluorescent probes for chemotherapy and phototherapy. *Coord Chem Rev* 2021;**427**:213556−67.
54. Liu Q, Sun Y, Yang T, Feng W, Li C, Li F. Sub-10 nm hexagonal lanthanide-doped $NaLuF_4$ upconversion nanocrystals for sensitive bioimaging *in vivo*. *J Am Chem Soc* 2011;**133**:17122−5.
55. Xie X, Gao N, Deng R, Sun Q, Xu QH, Liu X. Mechanistic investigation of photon upconversion in Nd^{3+}-sensitized core-shell nanoparticles. *J AmChem Soc* 2013;**135**:12608−11.
56. Lin Q, Huang Q, Li C, Bao C, Liu Z, Li F, et al. Anticancer drug release from a mesoporous silica based nanophotocage regulated by either a one- or two-photon process. *J Am Chem Soc* 2010;**132**:10645−7.
57. Shen J, Chen G, Vu AM, Fan W, Bilsel OS, Chang CC. Engineering the upconversion nanoparticle excitation wavelength: cascade sensitization of tri-doped upconversion colloidal nanoparticles at 800 nm. *Adv Opt Mater* 2013;**1**:644−50.
58. Kobayashi H, Ogawa M, Alford R, Choyke PL, Urano Y. New strategies for fluorescent probe design in medical diagnostic imaging. *Chem Rev* 2009;**110**:2620−40.
59. Kim A, Zhou J, Samaddar S, Song SH, Elzey BD, Thompson DH, et al. An implantable ultrasonically-powered micro-light-source (MLight) for photodynamic therapy. *Sci Rep* 2019;**9**:1395−403.
60. Tong R, Hemmati HD, Langer R, Kohane DS. Photoswitchable nanoparticles for triggered tissue penetration and drug delivery. *J Am Chem Soc* 2012;**134**:8848−55.
61. Ai1 X, Mu1 J, Xing B. Recent advances of light-mediated theranostics. *Theranostics* 2016;**6**:2439−57.

62. Falvey D, Sundararajan S. Photoremovable protecting groups based on electron transfer chemistry. *Photochem Photobiol Sci* 2004;**3**:831−8.
63. Singh PK, Majumdar P, Singh SP. Advances in BODIPY photocleavable protecting groups. *Coord Chem Rev* 2021;**449**:214193.
64. Pal DS, Kar H, Ghosh S. Phototriggered supramolecular polymerization. *Chemistry* 2016;**22**:16872−7.
65. Li P, Song Y, Dong CM. Hyperbranched polypeptides synthesized from phototriggered ROP of a photocaged *Nε*-[1-(2-nitrophenyl) ethoxycarbonyl]-l-lysine-*N*-carboxyanhydride: microstructures and effects of irradiation intensity and nitrogen flow rate. *Polym Chem* 2018;**9**:3974−86.
66. Schaal J, Dekowski B, Wiesner B, Eichhorst J, Marter K, Vargas C, et al. Coumarin-based octopamine phototriggers and their effects on an insect octopamine receptor. *Chembiochem* 2012;**13**:1458−64.
67. Bourbon P, Peng Q, Ferraudi G, Stauffacher C, Wiest O, Helquist P. Development of carbamate-tethered coumarins as phototriggers for caged nicotinamide. *Bioorg Med Chem Lett* 2013;**23**:6321−4.
68. Houk AL, Givens RS, Elles CG. Two-photon activation of *p*-hydroxyphenacyl phototriggers: toward spatially controlled release of diethyl phosphate and ATP. *J Phys Chem B* 2016;**120**:3178−86.
69. Ma C, Kwok WM, Chan WS, Du Y, Kan JTW, Toy PH, et al. Ultrafast time-resolved transient absorption and resonance raman spectroscopy study of the photodeprotection and rearrangement reactions of *p*-hydroxyphenacyl caged phosphates. *J Am Chem Soc* 2006;**128**:2558−70.
70. Wijtmans M, Rosenthal SJ, Zwanenburg B, Porter NA. Visible light excitation of CdSe nanocrystals triggers the release of coumarin from cinnamate surface ligands. *J Am Chem Soc* 2006;**128**:11720−6.
71. Duan XY, Zhai BC, Song QH. Water-soluble *o*-hydroxycinnamate as an efficient photoremovable protecting group of alcohols with fluorescence reporting. *Photochem Photobiol Sci* 2012;**11**:593−8.
72. Rajesh CS, Givens RS, Wirz J. Kinetics and mechanism of phosphate photorelease from benzoin diethyl phosphate: evidence for adiabatic fission to an α-keto cation in the triplet state. *J Am Chem Soc* 2000;**122**:611−8.
73. Dai XJ, Yu YQ, Liu KH, Su HM. Photochemical reaction of benzoin caged compound: time-resolved fourier transform infrared spectroscopy study. *Chin J Chem Phys* 2016;**29**:91−8.
74. McKay LJ, Carling C, Branda NR. Improved polyaromatic benzoin photoremovable protecting groups. *J Photochem Photobiol, A* 2021;**421**:113530−5.
75. Corrie JET, Furuta T, Givens RS, Yousef AL, Goeldner M. Photoremovable protecting groups used for the caging of biomolecules. In: Goeldner M, Givens RS, editors. *Dynamic studies in biology: phototriggers, photoswitches and caged biomolecules*. Wiley; 2005. p. 1−94.
76. Mayer G, Heckel A. Biologically active molecules with a "light switch". *Angew Chem Int Ed Engl* 2006;**45**:4900−21.
77. Zhang J, Zou Q, Tian H. Photochromic materials: more than meets the eye. *Adv Mater* 2013;**25**:378−99.
78. Zhu Y, Pavlos CM, Toscano JP, Dore TM. 8-Bromo-7-hydroxyquinoline as a photoremovable protecting group for physiological use: mechanism and scope. *J Am Chem Soc* 2006;**128**:4267−76.
79. Huang J, Muliawan AP, Ma J, Li MD, Chiu HK, Lan X, et al. A spectroscopic study of the excited state proton transfer processes of (8-bromo-7-hydroxyquinolin-2-yl)methyl-protected phenol in aqueous solutions. *Photochem Photobiol Sci* 2017;**16**:575−84.
80. Wang DD, Ge CW, Wu GA, Li ZP, Wang JZ, Zhang TF, et al. A sensitive red light nano-photodetector propelled by plasmonic copper nanoparticles. *J Mater Chem C* 2017;**5**:1328−35.
81. Ge D, Issa A, Jradi S, Couteau C, Marguet S, Bachelot R. Advanced hybrid plasmonic nano-emitters using smart photopolymer. *Photon Res* 2022;**10**:1552−66.
82. Roco MC, Bainbridge WS. *Converging technologies for improving human performance: nanotechnology, biotechnology, information technology and cognitive science*. Kluwer Academic Publishers; 2003.
83. Shamsipur M, Barati A, Nematifar Z. Fluorescent pH nanosensors: design strategies and applications. *J Photochem Photobiol C Photochem Rev* 2019;**39**:76−141.
84. Shamsipur M, Safavi A, Mohammadpour Z. Indirect colorimetric detection of glutathione based on its radical restoration ability using carbon nanodots as nanozymes. *Sensor Actuator B Chem* 2014;**199**:463−9.
85. Rostami E, Kashanian S, Azandaryani AH, Faramarzi H, Dolatabadi JEN, Omidfar K. Drug targeting using solid lipid nanoparticles. *Chem Phys Lipids* 2014;**181**:56−61.
86. Galangau O, Delbaere S, Ratel-Ramond N, Rapenne G, Li R, Calupitan JPDC, et al. Dual photochemical bond cleavage for a diarylethene-based phototrigger containing both methanolic and acetic sources. *J Org Chem* 2016;**81**:11282−90.
87. Li P, Liu K, Ye J, Xue F, Cheng Y, Lyu Z, et al. Facilitating the C−C bond cleavage on sub-10 nm concavity-tunable Rh@Pt core-shell nanocubes for efficient ethanol electrooxidation. *J Mater Chem* 2019;**7**:17987−94.
88. Kohman RE, Cha SS, Man HY, Han X. Light-triggered release of bioactive molecules from DNA nanostructures. *Nano Lett* 2016;**16**:2781−5.
89. Fan W, Bu W, Zhang Z, Shen B, Zhang H, He Q, et al. X-ray radiation-controlled NO-release for on-demand depth-independent hypoxic radiosensitization. *Angew Chem Int Ed Engl* 2015;**127**:14232−6.
90. Butcher DP, Rachford AA, Petersen JL, Rack JJ. Phototriggered S→O isomerization of a ruthenium-bound chelating sulfoxide. *Inorg Chem* 2006;**45**:9178−80.
91. Vittardi SB, Magar RT, Breen DJ, Rack JJ. A future perspective on phototriggered isomerizations of transition metal sulfoxides and related complexes. *J Am Chem Soc* 2021;**143**:526−37.
92. Olejniczak J, Carling CJ, Almutairi A. Photocontrolled release using one-photon absorption of visible or NIR light. *J Contr Release* 2015;**219**:18−30.
93. Biswas S, Rajesh Y, Barman S, Bera M, Paul A, Mandal M, et al. A dual-analyte probe: hypoxia activated nitric oxide detection with phototriggered drug release ability. *Chem Commun* 2018;**54**:7940−3.
94. Rogach AL, Franzl T, Klar TA, Feldmann J, Gaponik N, Lesnyak V, et al. Aqueous synthesis of thiol-capped CdTe nanocrystals: state-of-the-art. *J Phys Chem C* 2007;**111**:14628−37.
95. Xue Y, Liu D, Wang C, Bao C, Wang X, Zhu H, et al. Photo and reduction dual-responsive hydrogel for regulating cell adhesion and cell sheet harvest. *ACS Appl Bio Mater* 2020;**3**:2410−8.
96. Ruggiero E, Hernández-Gil J, Mareque-Rivas JC, Salassa L. Near infrared activation of an anticancer Pt^{IV} complex by Tm-doped upconversion nanoparticles. *Chem Commun* 2015;**5**:2091−4.
97. Wang Z, Yu L, Lv C, Wang P, Chen Y, Tang X. Photoresponsive cross-linked polymeric particles for phototriggered burst release. *Photochem Photobiol* 2013;**89**:552−9.
98. Cheawchan S, Sogawa H, Takata T. Phototriggered crosslinking and surface modification *via* catalyst-free functionalization of a new orthogonal agent containing nitrile *N*-oxide and *o*-nitrobenzyl ether moieties. *Macromol Chem Phys* 2021;**222**:2000459.
99. Tang S, Cannon J, Yang K, Krummel MF, Choi SK. Spacer-mediated control of coumarin uncaging for photocaged thymidine. *J Org Chem* 2020;**85**:2945−55.
100. Mahmoodi MM, Abate-Pella D, Pundsack TJ, Palsuledesai CC, Goff PC, Blank DA, Distefano MD. Nitrodibenzofuran: a one- and two-photon sensitive protecting group that is superior to brominated hydroxycoumarin for thiol caging in peptides. *J Am Chem Soc* 2016;**138**:5848−59.

101. Jana A, Atta S, Sarkar SK, Singh NDP. 1-Acetylpyrene with dual functions as an environment-sensitive fluorophore and fluorescent photoremovable protecting group. *Tetrahedron* 2010;**66**:9798−807.
102. Karthik S, Jana A, Selvakumar M, Venkatesh Y, Paul A, Shah SS, et al. Coumarin polycaprolactone polymeric nanoparticles: light and tumor microenvironment activated cocktail drug delivery. *J Mater Chem B* 2017;**5**:1734−41.
103. Gallo RDC, Duarte M, da Silva AF, Okada Jr CY, Deflon VM, Jurberg ID. A selective C−C bond cleavage strategy promoted by visible light. *Org Lett* 2021;**23**:8916−20.
104. Givens RS, Stensrud K, Conrad PG, Yousef AL, Perera C, Senadheera SN, et al. *p*-Hydroxyphenacyl photoremovable protecting groups-robust photochemistry despite substituent diversity. *Can J Chem* 2011;**89**:364−84.
105. Givens RS, Rubina M, Wirz J. Applications of *p*-hydroxyphenacyl (*p*HP) and coumarin-4-ylmethyl photoremovable protecting groups. *Photochem Photobiol Sci* 2012;**11**:472−88.
106. Givens RS, Weber JFW, Conrad PG, Orosz G, Donahue SL, Thayer SA. New phototriggers 9: *p*-hydroxylphenacyl as a C-terminal photoremovable protecting group for oligopeptides. *J Am Chem Soc* 2000;**122**:2687−97.
107. Givens RS, Park CH. *p*-Hydroxyphenacyl ATP1: a new phototrigger. *Tetrahedron Lett* 1996;**37**:6259−62.
108. Barman S, Mukhopadhyay SK, Biswas S, Nandi S, Gangopadhyay M, Dey S, et al. A *p*-hydroxyphenacyl-benzothiazole-chlorambucil conjugate as a real-time-monitoring drug-delivery system assisted by excited-state intramolecular proton transfer. *Angew Chem Int Ed* 2016;**55**:4194−8.
109. Singh AK, Kundu M, Roy S, Roy B, Shah SS, Nair AV, et al. Two-photon responsive napthyl tagged *p*-hydroxyphenacyl based drug delivery system: uncaging of anti-cancer drug in the phototherapeutic window with real-time monitoring. *Chem Commun* 2020;**56**:9986−9.
110. Wang H, Liu G. Advances in luminescent materials with aggregation-induced emission (AIE) properties for biomedical applications. *J Mater Chem B* 2018;**6**:4029−42.
111. Hu F, Xu S, Liu B. Photosensitizers with aggregation-induced emission: materials and biomedical applications. *Adv Mater* 2018;**30**:1801350−78.
112. Liang J, Tang BZ, Liu B. Specific light-up bioprobes based on AIEgen conjugates. *Chem Soc Rev* 2015;**44**:2798−811.
113. Denk W, Strickler JH, Webb WW. Two-photon laser scanning fluorescence microscopy. *Science* 1990;**248**:73−6.
114. Adams SR, Tsien RY. Controlling cell chemistry with caged compounds. *Annu Rev Physiol* 1993;**55**:755−84.
115. Bort G, Gallavardin T, Ogden D, Dalko PI. From one-photon to two-photon probes: "caged" compounds, actuators, and photoswitches. *Angew Chem Int Ed* 2013;**52**:4526−37.
116. Abe M, Chitose Y, Jakkampudi S, Thuy PTT, Lin Q, Van BT, et al. Design and synthesis of two-photon responsive chromophores for near-infrared light-induced uncaging reactions. *Synthesis* 2017;**49**:3337−46.
117. Chitose Y, Abe M. Design and synthesis of two-photon responsive chromophores for application to uncaging reactions. *Photochemistry* 2018;**46**:219241.
118. Jakkampudi S, Abe M. Caged compounds for two-photon uncaging. *Module Chem Mol Sci Chem Eng* 2018;**1**:1−11.
119. Klausen M, Blanchard-Desce M. Two-photon uncaging of bioactive compounds: starter guide to an efficient IR light switch. *J Photochem Photobiol C Photochem Rev* 2021;**48**:100423.
120. Alifu N, Dong X, Li D, Sun X, Zebibula A, Zhang D, et al. Aggregation-induced emission nanoparticles as photosensitizer for two-photon photodynamic therapy. *Mater Chem Front* 2017;**1**:1746−53.
121. Zhuang W, Xu Y, Li G, Hu J, Ma B, Yu T, et al. Redox and pH dual-responsive polymeric micelles with aggregation-induced emission feature for cellular imaging and chemotherapy. *ACS Appl Mater Interfaces* 2018;**10**:18489−98.
122. Feng HT, Yuan YX, Xiong JB, Zheng YS, Tang BZ. Macrocycles and cages based on tetraphenylethylene with aggregation-induced emission effect. *Chem Soc Rev* 2018;**47**:7452−76.
123. Jana A, Nguyen KT, Li X, Zhu P, Tan NS, Agren H, et al. Perylene-derived single-component organic nanoparticles with tunable emission: efficient anticancer drug carriers with real-time monitoring of drug release. *ACS Nano* 2014;**8**:5939−52.
124. Parthiban C, Pavithra M, Reddy VKL, Sen D, Samuel MS, Singh NDP. Visible light triggered fluorescent organic nanoparticles for chemo-photodynamic therapy with real time cellular imaging. *ACS Appl Nano Mater* 2018;**1**:6281−8.
125. Parthiban C, Pavithra M, Reddy LVK, Sen D, Singh NDP. Single-component fluorescent organic nanoparticles with four-armed phototriggers for chemo-photodynamic therapy and cellular imaging. *ACS Appl Nano Mater* 2019;**2**:3728−34.
126. Parthiban C, Pavithra M, Reddy LVK, Sen D, Samuel SM, Singh NDP. Tetraphenylethylene conjugated *p*-hydroxyphenacyl: fluorescent organic nanoparticles for the release of hydrogen sulfide under visible light with real-time cellular imaging. *Org Biomol Chem* 2018;**16**:7903−9.
127. Turner AD, Pizzo SV, Rozakis G, Porter NA. Photoreactivation of irreversibly inhibited serine proteinases. *J Am Chem Soc* 1988;**110**:244−50.
128. Li H, Yang J, Porter NA. Preparation and photochemistry of *o*-aminocinnamates. *J Photochem Photobiol, A* 2005;**169**:289−97.
129. Paul A, Mengji R, Chandy OA, Nandi S, Bera M, Jana A, et al. ESIPT-induced fluorescent *o*-hydroxycinnamate: a self-monitoring phototrigger for prompt image-guided uncaging of alcohols. *Org Biomol Chem* 2017;**17**:8544−855.
130. Abdallah M, Hijazi A, Dumur F, Lalevée J. Coumarins as powerful photosensitizers for the cationic polymerization of epoxy-silicones under near-UV and visible light and applications for 3D printing technology. *Molecules* 2020;**25**:2063−75.
131. Ji PW, Li N, Chen D, Qi X, Sha W, Jiao Y, et al. Coumarin-containing photo-responsive nanocomposites for NIR light-triggered controlled drug release *via* a two-photon process. *J Mater Chem B* 2013;**1**:5942−9.
132. Huang Q, Bao C, Ji W, Wang Q, Zhu L. Photocleavable coumarin crosslinkers based polystyrene microgels: phototriggered swelling and release. *J Mater Chem* 2012;**22**:18275−82.
133. Trenor SR, Shultz AR, Love BJ, Long TE. Coumarins in polymers: from light harvesting to photo-cross-linkable tissue scaffolds. *Chem Rev* 2004;**104**:3059−78.
134. Maddipatla MVSN, Wehrung D, Tang C, Fan W, Oyewumi MO, Miyoshi T, et al. Photoresponsive coumarin polyesters that exhibit cross-linking and chain scission properties. *Macromolecules* 2013;**46**:5133−40.
135. Lin Q, Bao C, Cheng S, Yang Y, Ji W, Zhu L. Target-activated coumarin phototriggers specifically switch on fluorescence and photocleavage upon bonding to thiol-bearing protein. *J Am Chem Soc* 2012;**134**:5052−5.
136. Lin Q, Bao C, Yang Y, Liang Q, Zhang D, Cheng S, et al. Highly discriminating photorelease of anticancer drugs based on hypoxia activatable phototrigger conjugated chitosan nanoparticles. *Adv Mater* 2013;**25**:1981−6.
137. Beauté L, McClenaghan N, Lecommandoux S. Photo-triggered polymer nanomedicines: from molecular mechanisms to therapeutic applications. *Adv Drug Deliv Rev* 2019;**138**:148−66.
138. Olson JP, Kwon HB, Takasaki KT, Chiu CQ, Higley MJ, Sabatini BL, et al. Optically selective two-photon uncaging of glutamate at 900 nm. *J Am Chem Soc* 2013;**135**:5954−7.
139. Fournier L, Aujard I, LeSaux T, Maurin S, Beaupierre S, Baudin JB, et al. Coumarinyl methyl caging groups with redshifted absorption. *Chem Eur J* 2013;**19**:17494−507.
140. Chitose Y, Abe M, Furukawa K, Katan C. Design, synthesis, and reaction of -extended coumarin-based new caged compounds with two-photon absorption character in the near-IR region. *Chem Lett* 2016;**45**:1186−8.

141. Schiedel MS, Briehn CA, Bauerle P. Single-compound libraries of organic materials: parallel synthesis and screening of fluorescent dyes. *Angew Chem Int Ed* 2001;**40**:4677−80.
142. Yu J, Shirota Y. A new class of high-performance red-fluorescent dyes for organic electroluminescent devices, [7-diethylamino-3-(2-thienyl)chromen-2-ylidene]-2,2-dicyanovinylamineand{10-(2-thienyl)-2,3,6,7-tetrahydro-1*H*,5*H*-chromeno[8,7,6-*ij*]quinolizin-11-ylidene}-2,2-dicyanovinylamine. *Chem Lett* 2002;**31**:984−5.
143. Gandioso A, Contreras S, Melnyk I, Oliva J, Nonell S, Velasco D, et al. Development of green/red-absorbing chromophores based on a coumarin scaffold that are useful as caging groups. *J Org Chem* 2017;**82**:5398−408.
144. Wang BY, Lin YC, Lai YT, Ou JY, Chang WW, Chu CC. Targeted photoresponsive carbazole-coumarin and drug conjugates for efficient combination therapy in leukemia cancer cells. *Bioorg Chem* 2020;**100**:103904−11.
145. Klausen M, Dubois V, Clermont G, Tonnelé C, Castet F, Blanchard-Desce M. Dual-wavelength efficient two-photon photorelease of glycine by p-extended dipolar coumarins. *Chem Sci* 2019;**10**:4209−19.
146. Bojtar M, Nemeth K, Domahidy F, Knorr G, Verkman A, Kallay M, et al. Conditionally activatable visible-light photocages. *J Am Chem Soc* 2020;**142**:15164−71.
147. Kim E, Koo H. Biomedical applications of copper-free click chemistry: *in vitro, in vivo*, and *ex vivo*. *Chem Sci* 2019;**10**:7835−51.
148. Kozma E, Girona GE, Paci G, Lemke EA, Kele P. Bioorthogonal double-fluorogenic siliconrhodamine probes for intracellular super-resolution microscopy. *Chem Commun* 2017;**53**:6696−9.
149. Kormos A, Kern D, Egyed A, Soveges B, Nemeth K, Kele P. Microscope laser assisted photooxidative activation of bioorthogonal clickox probes. *Chem Commun* 2020;**56**:5425−8.
150. Knorr G, Kozma E, Schaart JM, Nemeth K, Torok G, Kele P. Bioorthogonally applicable fluorogenic cyanine-tetrazines for no-wash super-resolution imaging. *Bioconjugate Chem* 2018;**29**:1312−8.
151. Versteegen RM, tenHoeve W, Rossin R, deGeus MAR, Janssen HM, Robillard MS. Click-to-release from *trans*-cyclooctenes: mechanistic insights and expansion of scope from established carbamate to remarkable ether cleavage. *Angew Chem Int Ed* 2018;**57**:10494−9.
152. Werther P, Yserentant K, Braun F, Kaltwasser N, Popp C, Baalmann M, et al. Live-cell localization microscopy with a fluorogenic and self-blinking tetrazine probe. *Angew Chem Int Ed* 2020;**59**:804−10.
153. Wçll D, Smirnova J, Galetskaya M, Prykota T, Buhler J, Stengele KP, et al. Intramolecular sensitization of photocleavage of the photolabile 2-(2-nitrophenyl)propoxycarbonyl (NPPOC) protecting group: photoproducts and photokinetics of the release of nucleosides. *Chem Eur J* 2008;**14**:6490−7.
154. Mbatia HW, Bandara HMD, Burdette SC. Cupro Cleav-1, a first generation photocage for Cu^{+}. *Chem Commun* 2012;**48**:5331−3.
155. Donato L, Mourot A, Davenport CM, Herbivo C, Warther D, Leonard J, et al. Water-soluble, donor-acceptor biphenyl derivatives in the 2-(*o*-nitrophenyl)propyl series: highly efficient two-photon uncaging of the neurotransmitter γ-aminobutyric acid at $\lambda = 800$ nm. *Angew Chem Int Ed* 2012;**51**:1840−3.
156. Walbert S, Pfleiderer W, Steiner UE. Photolabile protecting groups for nucleosides: mechanistic studies of the 2-(2-nitrophenyl)ethyl group. *Helv Chim Acta* 2001;**84**:1601−11.
157. Wang X, Yang Y, Liu C, Guo H, Chen Z, Xia J, et al. Photo- and pH-responsive drug delivery nanocomposite based on *o*-nitrobenzyl functionalized upconversion nanoparticles. *Polymer* 2021;**229**:123961−9.
158. Monteiro DCF, Amoah E, Rogers C, Pearson AR. Using photocaging for fast time-resolved structural biology studies. *Acta Crystallogr D Struct Biol* 2021;**77**:1218−32.
159. Carling CJ, Viger ML, Huu VAN, Garcia AV, Almutairi A. *In vivo* visible light-triggered drug release from an implanted depot. *Chem Sci* 2015;**6**:335−41.
160. Olejniczak J, Sankaranarayanan J, Viger ML, Almutairi A. Highest efficiency two-photon degradable copolymer for remote controlled release. *ACS Macro Lett* 2013;**2**:683−7.
161. Sun S, Chamsaz EA, Joy A. Photoinduced polymer chain scission of alkoxyphenacyl based polycarbonates. *ACS Macro Lett* 2012;**1**:1184−8.
162. Yuan X, Wang B, Yang L, Zhang Y. The role of ROS-induced autophagy in hepatocellular carcinoma. *Clin Res Hepatol Gastroenterol* 2018;**42**:306−12.
163. Qi S, Guo L, Yan S, Lee RJ, Yu S, Chen S. Hypocrellin A-based photodynamic action induces apoptosis in A549 cells through ROS-mediated mitochondrial signaling pathway. *Acta Pharm Sin B* 2019;**9**:279−93.
164. Liou GY, Storz P. Reactive oxygen species in cancer. *Free Radic Res* 2010;**44**:479−96.
165. Gong H, Chao Y, Xiang J, Han X, Song G, Feng L, et al. Hyaluronidase to enhance nanoparticle-based photodynamic tumor therapy. *Nano Lett* 2016;**16**:2512−21.
166. Liu B, Li C, Cheng Z, Hou Z, Huang S, Lin J. Functional nanomaterials for near-infrared-triggered cancer therapy. *Biomater Sci* 2016;**4**:890−909.
167. Yue C, Zhang C, Alfranca G, Yang Y, Jiang X, Yang Y, et al. Near-infrared light triggered ROS-activated theranostic platform based on Ce6-CPT-UCNPs for simultaneous fluorescence imaging and chemo-photodynamic combined therapy. *Theranostics* 2016;**6**:456−69.
168. Tapeinos C, Pandit A. Physical, chemical, and biological structures based on ROS-sensitive moieties that are able to respond to oxidative microenvironments. *Adv Mater* 2016;**28**:5553−85.
169. Nguyen VN, Ha J, Cho M, Li H, Swamy KMK, Yoon J. Recent developments of BODIPY-based colorimetric and fluorescent probes for the detection of reactive oxygen/nitrogen species and cancer diagnosis. *Coord Chem Rev* 2021;**439**:213936−53.
170. Shi S, Zhang L, Zhu M, Wan G, Li C, Zhang J, et al. Reactive oxygen species-responsive nanoparticles based on peglated prodrug for targeted treatment of oral tongue squamous cell carcinoma by combining photodynamic therapy and chemotherapy. *ACS Appl Mater Interfaces* 2018;**10**:29260−72.
171. Saravanakumar G, Kim J, Kim WJ. Reactive-oxygen-species-responsive drug delivery systems: promises and challenges. *Adv Sci* 2017;**4**:1600124−43.
172. Jin H, Zhu T, Huang X, Sun M, Li H, Zhu X, et al. ROS-responsive nanoparticles based on amphiphilic hyperbranched polyphosphoester for drug delivery: light-triggered size-reducing and enhanced tumor penetration. *Biomaterials* 2019;**211**:68−80.
173. Rapp TL, DeForest CA. Targeting drug delivery with light: a highly focused approach. *Adv Drug Deliv Rev* 2021;**171**:94−107.
174. Kuncewicz J, Dąbrowski JM, Kyzioł A, Brindell M, Łabuz P, Mazuryk O, et al. Perspectives of molecular and nanostructured systems with d- and f-block metals in photogeneration of reactive oxygen species for medical strategies. *Coord Chem Rev* 2019;**398**:113012−43.
175. Detty MR, Gibson SL, Wagner SJ. Current clinical and preclinical photosensitizers for use in photodynamic therapy. *J Med Chem* 2004;**47**:3897−915.
176. Konan YN, Gurny R, Allémann E. State of the art in the delivery of photosensitizers for photodynamic therapy. *J Photochem Photobiol B Biol* 2002;**66**:89−106.
177. Chen B, Zhang Y, Ran R, Wang B, Qin F, Zhang T, et al. Reactive oxygen species-responsive nanoparticles based on thioketal-containing poly(β-amino ester) for combining photothermal/photodynamic therapy and chemotherapy. *Polym Chem* 2019;**10**:4746−57.
178. Men Y, Brevé TG, Liu H, Denkova AG, Eelkema R. Photo cleavable thioacetal block copolymers for controlled release. *Polym Chem* 2021;**12**:3612−8.
179. Shen Y, Xu C, Chen J, Guan Z, Huang Y, Zeng Z, et al. Photo-triggered self-adaptive functionalized moc-based drug delivery

platform promises high antitumor efficacy. *Adv Healthcare Mater* 2021;**1**:2100676−87.
180. Bloch WM, Clever GH. Integrative self-sorting of coordination cages based on 'naked' metal ions. *Chem Commun* 2017;**53**:8506−16.
181. Beuerle F, Gole B. Covalent organic frameworks and cage compounds: design and applications of polymeric and discrete organic scaffolds. *Angew Chem Int Ed* 2018;**57**:4850−78.
182. Hiraoka S, Kubota Y, Fujita M. Self- and hetero-recognition in the guest-controlled assembly of Pd(II)-linked cages from two different ligands. *Chem Commun* 2000;**1**:1509−10.
183. Kumazawa K, Biradha K, Kusukawa T, Okano T, Fujita M. Multicomponent assembly of a pyrazine-pillared coordination cage that selectively binds planar guests by intercalation. *Angew Chem Int Ed* 2003;**42**:3909−13.
184. Yamashina M, Yuki T, Sei Y, Akita M, Yoshizawa M. Anisotropic expansion of an M2L4 coordination capsule: host capability and frame rearrangement. *Chem Eur J* 2015;**21**:4200−4.
185. Sun QF, Sato S, Fujita M. An $M_{12}(L^1)_{12}(L^2)_{12}$ cantellated tetrahedron: a case study on mixed-ligand self-assembly. *Angew Chem Int Ed* 2014;**53**:13510−3.
186. Bloch WM, Abe Y, Holstein JJ, Wandtke CM, Dittrich B, Clever GH. Geometric complementarity in assembly and guest recognition of a bent heteroleptic *cis*-[$Pd_2LA_2LB_2$] coordination cage. *J Am Chem Soc* 2016;**138**:13750−5.
187. Bloch WM, Holstein JJ, Hiller W, Clever GH. Morphological control of heteroleptic *cis*- and *trans*-$Pd_2L_2L'_2$ cages. *Angew Chem Int Ed* 2017;**56**:8285−9.
188. Li JR, Zhou HC. Bridging-ligand-substitution strategy for the preparation of metal-organic polyhedral. *Nat Chem* 2010;**2**:893−8.
189. Feng L, Wang KY, Day GS, Zhou HC. The chemistry of multicomponent and hierarchical framework compounds. *Chem Soc Rev* 2019;**48**:4823−53.
190. Zhu W, Guo J, Ju Y, Serda RE, Croissant JG, Shang J, et al. Modular metal-organic polyhedra superassembly: from molecular-level design to targeted drug delivery. *Adv Mater* 2019;**31**:1806774−83.
191. Zhang X, Dong X, Lu W, Luo D, Zhu XW, Li X, et al. Fine-tuning apertures of metal-organic cages: encapsulation of carbon dioxide in solution and solid state. *J Am Chem Soc* 2019;**141**:11621−7.
192. Nihei M, Ida H, Nibe T, Moeljadi AMP, Trinh QT, Hirao H, et al. Ferrihydrite particle encapsulated within a molecular organic cage. *J Am Chem Soc* 2018;**140**:17753−9.
193. Gosselin EJ, Rowland CA, Bloch ED. Permanently microporous metal-organic polyhedra. *Chem Rev* 2020;**120**:8987−9014.
194. Chen Z, Chen B, He M, Wang H, Hu B. A porous organic polymer with magnetic nanoparticles on a chip array for preconcentration of platinum(IV), gold(III) and bismuth(III) prior to their on-line quantitation by ICP-MS. *Mikrochim Acta* 2019;**186**:107−14.
195. Das S, Heasman P, Ben T, Qiu S. Porous organic materials: strategic design and structure-function correlation. *Chem Rev* 2017;**117**:1515−63.
196. Pan M, Wu K, Zhang JH, Su CY. Chiral metal-organic cages/containers (MOCs): from structural and stereochemical design to applications. *Coord Chem Rev* 2019;**378**:333−49.
197. Gao Y, Deng SQ, Jin X, Cai SL, Zheng SR, Zhang WG. The construction of amorphous metal-organic cage-based solid for rapid dye adsorption and time-dependent dye separation from water. *Chem Eng J* 2019;**357**:129−39.
198. An Y, Zhu J, Liu F, Deng J, Meng X, Liu G, et al. Boosting the ferroptotic antitumor efficacy *via* site-specific amplification of tailored lipid peroxidation. *ACS Appl Mater Interfaces* 2019;**11**:29655−66.
199. Li HJ, Du JZ, Liu J, Du XJ, Shen S, Zhu YH, et al. Smart superstructures with ultrahigh pH-sensitivity for targeting acidic tumor microenvironment: instantaneous size switching and improved tumor penetration. *ACS Nano* 2016;**10**:6753−61.
200. Johnson AM, Hooley RJ. Steric effects control self-sorting in self-assembled clusters. *Inorg Chem* 2011;**50**:4671−3.
201. Preston D, Barnsley JE, Gordon KC, Crowley JD. Controlled formation of heteroleptic $[Pd_2(La)_2(Lb)_2]^{(4+)}$ cages. *J Am Chem Soc* 2016;**138**:10578−85.
202. Zheng YR, Zhao ZG, Wang M, Ghosh K, Pollock JB, Cook TR, et al. A facile approach toward multicomponent supramolecular structures: selective self-assembly *via* charge separation. *J Am Chem Soc* 2010;**132**:16873−82.
203. Kabb CP, O'Bryan CS, Morley CD, Angelini TE, Sumerlin BS. Anthracene-based mechanophores for compression-activated fluorescence in polymeric networks. *Chem Sci* 2019;**10**:7702−8.
204. Syrett JA, Mantovani G, Barton WRS, Price D, Haddleton DM. Self-healing polymers prepared *via* living radical polymerization. *Polym Chem* 2010;**1**:102−6.
205. Li J, Shiraki T, Hu B, Wright RAE, Zhao B, Moore JS. Mechanophore activation at heterointerfaces. *J Am Chem Soc* 2014;**136**:15925−8.
206. Church DC, Peterson GI, Boydston AJ. Comparison of mechanochemical chain scission rates for linear *versus* three-arm star polymers in strong acoustic fields. *ACS Macro Lett* 2014;**3**:648−51.
207. Li H, Gostl R, Delgove M, Sweeck J, Zhang Q, Sijbesma RP, et al. Promoting mechanochemistry of covalent bonds by noncovalent micellar aggregation. *ACS Macro Lett* 2016;**5**:995−8.
208. Sun H, Kabb CP, Dai Y, Hill MR, Ghiviriga I, Bapat AP, et al. Macromolecular metamorphosis *via* stimulus-induced transformations of polymer architecture. *Nat Chem* 2017;**9**:817−23.
209. Wang J, Piskun I, Craig SL. Mechanochemical strengthening of a multi-mechanophore benzocyclobutene polymer. *ACS Macro Lett* 2015;**4**:834−7.
210. Gordon MB, Wang S, Knappe GA, Wagner NJ, Epps TH, Kloxin CJ. Force-induced cleavage of a labile bond for enhanced mechanochemical crosslinking. *Polym Chem* 2017;**8**:6485−9.
211. Chen Z, Mercer JAM, Zhu X, Romaniuk JAH, Pfattner R, Cegelski L, et al. Mechanochemical unzipping of insulating polyladderene to semiconducting polyacetylene. *Science* 2017;**357**:475−9.
212. Larsen MB, Boydston AJ. "Flex-activated" mechanophores: using polymer mechanochemistry to direct bond bending activation. *J Am Chem Soc* 2013;**135**:8189−92.
213. Cao B, Boechler N, Boydston AJ. Additive manufacturing with a flex activated mechanophore for nondestructive assessment of mechanochemical reactivity in complex object geometries. *Polymer* 2018;**152**:4−8.
214. Gossweiler GR, Hewage GB, Soriano G, Wang Q, Welshofer GW, Zhao X, et al. Mechanochemical activation of covalent bonds in polymers with full and repeatable macroscopic shape recovery. *ACS Macro Lett* 2014;**3**:216−9.
215. Peterson GI, Larsen MB, Ganter MA, Storti DW, Boydston AJ. 3D-Printed mechanochromic materials. *ACS Appl Mater Interfaces* 2015;**7**:577−83.
216. Song X, Song Y, Cui X, Wang JP, Luo Y, Qi T, et al. Intrinsic healable mechanochromic materials *via* incorporation of spiropyran mechanophore into polymer main chain. *Polymer* 2022;**250**:124878.
217. Larsen MB, Boydston AJ. Successive mechanochemical activation and small molecule release in an elastomeric material. *J Am Chem Soc* 2014;**136**:1276−9.
218. Cheng CC, Huang JJ, Lee AW, Huang SY, Huang CY, Lai JY. Highly effective photocontrollable drug delivery systems based on ultrasensitive light-responsive self-assembled polymeric micelles: an *in vitro* therapeutic evaluation. *ACS Appl Bio Mater* 2019;**2**:2162−70.
219. Cardano F, Canto ED, Giordani S. Spiropyran for light-controlled drug delivery. *Dalton Trans* 2019;**48**:15537−44.
220. Cheng H, Yoon J, Tian H. Recent advances in the use of photochromic dyes for photocontrol in biomedicine. *Coord Chem Rev* 2018;**372**:66−84.
221. Velema WA, Szymanski W, Feringa BL. Photopharmacology: beyond proof of principle. *J Am Chem Soc* 2014;**136**:2178−91.

222. Cheng HB, Zhang S, Qi J, Liang XJ, Yoon J. Advances in application of azobenzene as a trigger in biomedicine: molecular design and spontaneous assembly. *Adv Mater* 2021;**1**:2007290−331.
223. Liu J, Bu W, Pan L, Shi PJ. NIR-triggered anticancer drug delivery by upconverting nanoparticles with integrated azobenzene-modified mesoporous silica. *Angew Chem Int Ed* 2013;**52**:4375−9.
224. Peddie V, Abell AD. Photocontrol of peptide secondary structure through non-azobenzene photoswitches. *J Photochem Photobiol C Photochem Rev* 2019;**40**:1−20.
225. Wang X, Hu J, Liu G, Tian J, Wang H, Gong M, et al. Reversibly switching bilayer permeability and release modules of photochromic polymersomes stabilized by cooperative noncovalent interactions. *J Am Chem Soc* 2015;**137**:15262−75.
226. Pavlukhina S, Sukhishvili S. Polymer assemblies for controlled delivery of bioactive molecules from surfaces. *Adv Drug Deliv Rev* 2011;**63**:822−36.
227. Volodkin DV, Madaboosi N, Blacklock J, Skirtach AG. Surface-supported multilayers decorated with bio-active material aimedat light-triggered drug delivery. *Langmuir* 2009;**25**:14037−43.
228. Marturano V, Cerruti P, Cerruti P, Giamberini M, Tylkowski B, Ambrogi V. Light-responsive polymer micro- and nano-capsules. *Polymers* 2017;**9**:8−26.
229. Görner H, Kuhn HJ. *Cis-trans* photoisomerization of stilbenes and stilbene-like molecules. In: Neckers DC, Volman DH, von Bünau G, editors. *Advance in photochemistry*. Hoboken: John Wiley & Sons, Inc.; 1994.
230. Granados A, Vallribera A. Fluorous hydrophobic fluorescent (*E*)-stilbene derivatives for application on security paper. *Dyes Pigments* 2019;**170**:107597−608.
231. Abdollahi A, Sahandi-Zangabad K, Roghani-Mamaqani H. Rewritable anticounterfeiting polymer inks based on functionalized stimuli-responsive latex particles containing spiropyran photoswitches: reversible photopatterning and security marking. *ACS Appl Mater Interfaces* 2018;**10**:39279−92.
232. Abdollahi A, Mouraki A, Sharifian MH, Mahdavian AR. Photochromic properties of stimuli-responsive cellulosic papers modified by spiropyran-acrylic copolymer in reusable pH-sensors. *Carbohydr Polym* 2018;**200**:583−94.
233. Li E, Kang J, Ye P, Zhang W, Cheng F, Yin C. A prospective material for the highly selective extraction of lithium ions based on a photochromic crowned spirobenzopyran. *J Mater Chem B* 2019;**7**:903−7.
234. Sakai H, Ebana H, Sakai K, Tsuchiya K, Ohkubo T, Abe M. Photoisomerization of spiropyran-modified cationic surfactants. *J Colloid Interface Sci* 2007;**316**:1027−30.
235. Sahoo PR, Prakash K, Kumar S. Light controlled receptors for heavy metal ions. *Coord Chem Rev* 2018;**357**:18−49.
236. Ranjan P, Kumar SS. Photochromic spirooxazine as highly sensitive and selective probe for optical detection of Fe^{3+} in aqueous solution. *Sensor Actuator B Chem* 2016;**226**:548−52.
237. Sun B, He Z, Hou Q, Liu Z, Cha R, Ni Y. Interaction of a spirooxazine dye with latex and its photochromic efficiency on cellulosic paper. *Carbohydr Polym* 2013;**95**:598−605.
238. Guerchais V, Ordronneau L, Bozec HL. Recent developments in the field of metal complexes containing photochromic ligands: modulation of linear and nonlinear optical properties. *Coord Chem Rev* 2010;**254**:2533−45.
239. Li Z, Liu Y, Yang XG, Gao X, Zhang Y, Zhang H, et al. Cyanostilbene-functionalized dithienylethenes with aggregation -induced emission for photoswitching behavior in multi-media. *J Lumin* 2022;**250**:119061.
240. Yan Q, Qiao Z, Xu J, Ren J, Wang S. All-visible-light triggered photochromic fluorescent dithienylethene-phenanthroimidazole dyads: synthesis, crystal structure, multiple switching behavior and information storage. *Dyes Pigments* 2022;**202**:110298.
241. Zhang H, Qi Y, Zhao X, Li M, Wang R, Cheng H, et al. Dithienylethene-bridged fluoroquinolone derivatives for imaging-guided reversible control of antibacterial activity. *J Org Chem* 2022;**87**:7446−55.
242. Huang Y, Dong R, Zhu X, Yan D. Photo-responsive polymeric micelles. *Soft Matter* 2014;**10**:6121−38.
243. Yuan Q, Zhang Y, Chen T, Lu D, Zhao Z, Zhang X, et al. Photon-manipulated drug release from a mesoporous nanocontainer controlled by azobenzene-modified nucleic acid. *ACS Nano* 2012;**7**:6337−44.
244. Tong X, Wang G, Soldera A, Zhao Y. How can azobenzene block copolymer vesicles be dissociated and reformed by light?. *J Phys Chem B* 2005;**109**:20281−7.
245. Jiang J, Tong X, Morris D, Zhao Y. Toward photocontrolled release using light-dissociable block copolymer micelles. *Macromolecules* 2006;**39**:4633−40.
246. Liu X, He J, Niu Y, Li Y, Hu D, Xia X, et al. Photo-responsive amphiphilic poly(α-hydroxy acids) with pendent *o*-nitrobenzyl ester constructed *via* copper-catalyzed azide-alkyne cycloaddition reaction. *Polym Adv Technol* 2015;**26**:449−56.
247. Shamsipur M, Ghavidast A. Facile synthesis of magnetic photo-responsive nanoparticles based on 1,3-diazabicyclo[3.1.0]hex-3-en: an enhanced adsorption of toxic dyes from aqueous solution under sunlight. *J Mol Struct* 2022;**263**:133130−43.
248. Mahmoodi NO, Ahmadi NK, Ghavidast A. Light-induced switching of 1,3-di-azabicyclo-[3.1.0]hex-3-enes on gold nanoparticles. *J Mol Struct* 2018;**1160**:463−70.
249. Mahmoodi NO, Ghavidast A, Mirkhaef S, Zanjanchi MA. Photochromism of azobenzene-thiol-1,3-diazabicyclo-[3.1.0]hex-3-ene on silver nanoparticles. *Dyes Pigments* 2015;**118**:110−7.
250. Fasihi-Ramandi M, Mahmoodi NO, Ghavidast A, Shirini F, Nahzomi HT. Synthesis and exploring the excited-state PES of photochromic hydrogen bond-assembled [2]rotaxane based on 1,3-diazabicyclo-[3.1.0]hex-3-enes. *Res Chem Intermed* 2021;**47**:1−16.
251. Ghavidast A, Mahmoodi NO, Zanjanchi MA. Synthesis and photochromicproperties of a novel thiol-terminated 1,3-diazabicyclo [3.1.0]hex-3-ene on silver nanoparticles. *J Mol Struct* 2013;**1048**:166−71.
252. Rad JK, Balzade Z, Mahdavian AR. Spiropyran-based advanced photoswitchable materials: a fascinating pathway to the future stimuli-responsive devices. *J Photochem Photobiol C Photochem Rev* 2022;**51**:100487.
253. ter Schiphorst J, Coleman S, Stumpel JE, Azouz AB, Diamond D, Schenning APHJ. Molecular design of light-responsive hydrogels, for *in situ* generation of fast and reversible valves for microfluidic applications. *Chem Mater* 2015;**27**:5925−31.
254. Zhang QM, Wang W, Su YQ, Hensen EJM, Serpe MJ. Biological imaging and sensing with multiresponsive microgels. *Chem Mater* 2016;**28**:259−65.
255. Zhu MQ, Zhu L, Han JJ, Wu W, Hurst JK, Li ADQ. Spiropyran-based photochromic polymer nanoparticles with optically switchable luminescence. *J Am Chem Soc* 2006;**128**:4303−9.
256. Li M, Zhang Q, Zhou YN, Zhu S. Let spiropyran help polymers feel force. *Prog Polym Sci* 2018;**79**:26−39.
257. Lee HI, Wu W, Oh JK, Mueller L, Sherwood G, Peteanu L, et al. Light-induced reversible formation of polymeric micelles. *Angew Chem Int Ed* 2007;**46**:2453−7.
258. Jochum FD, Theato P. Temperature- and light-responsive smart polymer materials. *Chem Soc Rev* 2013;**42**:7468−83.
259. Jochum FD, Theato P. Temperature- and light-responsive polyacrylamides prepared by a double polymer analogous reaction of activated ester polymers. *Macromolecules* 2009;**42**:5941−5.
260. Minkin VI. Photo-, thermo-, solvato-, and electrochromic spiroheterocyclic compounds. *Chem Rev* 2004;**104**:2751−76.
261. Berkovic G, Krongauz V, Weiss V. Spiropyrans and spirooxazines for memories and switches. *Chem Rev* 2000;**100**:1741−54.
262. Weissleder R. A clearer vision for *in vivo* imaging: progress continues in the development of smaller, more penetrable probes for biological imaging. *Nat Biotechnol* 2001;**19**:316−7.

263. Cho HJ, Chung M, Shim MS. Engineered photo-responsive materials for near-infrared-triggered drug delivery. *J Ind Eng Chem* 2015;**31**:15−25.
264. Linsley CS, Wu BM. Recent advances in light-responsive on-demand drug-delivery systems. *Ther Deliv* 2017;**8**:89−107.
265. Ghani M, Heiskanen A, Kajtez J, Rezaei B, Larsen NB, Thomsen P, et al. On-demand reversible UV-triggered interpenetrating polymer network-based drug delivery system using the spiropyran-merocyanine hydrophobicity switch. *ACS Appl Mater Interfaces* 2021;**13**:3591−604.
266. Tang Y, Wang G. NIR light-responsive nanocarriers for controlled release. *J Photochem Photobiol C Photochem Rev* 2021;**47**:100420−35.
267. Tylkowski B, Trojanowska A, Marturano V, Nowak M, Marciniak L, Giamberini M, et al. Power of light-functional complexes based on azobenzene molecules. *Coord Chem Rev* 2017;**351**:205−17.
268. Wang D, Wu S. Red-light-responsive supramolecular valves for photocontrolled drug release from mesoporous nanoparticles. *Langmuir* 2016;**32**:632−6.
269. Hartley GS. The *cis*-form of azobenzene. *Nature* 1937;**140**:281−2.
270. Yang H, Yuan B, Zhang X. Supramolecular chemistry at interfaces: host-guest interactions for fabricating multifunctional biointerfaces. *Acc Chem Res* 2014;**47**:2106−15.
271. Deng J, Liu X, Shi W, Cheng C, He C, Zhao C. Light-triggered switching of reversible and alterable biofunctionality *via* β-cyclodextrin/azobenzene-based host-guest interaction. *ACS Macro Lett* 2014;**3**:1130−3.
272. Shen Q, Liu L, Zhang W. Fabrication of a photocontrolled surface with switchable wettability based on host-guest inclusion complexation and protein resistance. *Langmuir* 2014;**30**:9361−9.
273. Wan P, Chen Y, Xing Y, Chi L, Zhang X. Combining host-guest systems with nonfouling material for the fabrication of a biosurface: toward nearly complete and reversible resistance of cytochrome *c*. *Langmuir* 2010;**26**:12515−7.
274. Becker D, Konnertz N, Böhning M, Schmidt J, Thomas A. Light-switchable polymers of intrinsic microporosity. *Chem Mater* 2016;**28**:8523−9.
275. Robertus J, Browne WR, Feringa BL. Dynamic control over cell adhesive properties using molecular-based surface engineering strategies. *Chem Soc Rev* 2010;**39**:354−78.
276. Szymanski W, Beierle JM, Kistemaker HAV, Velema WA, Feringa BL. Reversible photocontrol of biological systems by the incorporation of molecular photoswitches. *Chem Rev* 2013;**113**:6114−78.
277. Beharry AA, Woolley GA. Azobenzene photoswitches for biomolecules. *Chem Soc Rev* 2011;**40**:4422−37.
278. Merino E, Ribagorda M. Control over molecular motion using the *cis-trans* photoisomerization of the azo group. *Beilstein J Org Chem* 2012;**8**:1071−90.
279. Bandara HM, Burdette SC. Photoisomerization in different classes of azobenzene. *Chem Soc Rev* 2012;**41**:1809−25.
280. Weis P, Wu S. Light-switchable azobenzene-containing macromolecules: from UV to near infrared. *Macromol Rapid Commun* 2018;**39**:1700220−31.
281. Broichhagen J, Frank JA, Trauner D. A roadmap to success in photopharmacology. *Acc Chem Res* 2015;**48**:1947−60.
282. Qu DH, Wang QC, Zhang QW, Ma X, Tian H. Photoresponsive host-guest functional Systems. *Chem Rev* 2015;**115**:7543−88.
283. Han Y, Meng Z, Ma YX, Chen CF. Iptycene-derived crown ether hosts for molecular recognition and self-assembly. *Acc Chem Res* 2014;**47**:2026−40.
284. Mathapa BG, Paunov VN. Self-assembly of cyclodextrin-oil inclusion complexes at the oil-water interface: a route to surfactant-free emulsions. *J Mater Chem* 2013;**1**:10836−46.
285. Zhao Y, Huang Y, Zhu H, Zhu Q, Xia Y. Three-in-one: sensing, self-assembly, and cascade catalysis of cyclodextrin modified gold nanoparticles. *J Am Chem Soc* 2016;**138**:16645−54.
286. Yang S, Yan Y, Huang J, Petukhov AV, Kroon-Batenburg LMJ, Drechsler M, et al. Giant capsids from lattice self-assembly of cyclodextrin complexes. *Nat Commun* 2017;**8**:15856−62.
287. Yan H, Qiu Y, Wang J, Jiang Q, Wang H, Liao Y, et al. Wholly, visible-light-responsive host-guest supramolecular gels based on methoxy azobenzene and β-cyclodextrin dimmers. *Langmuir* 2020;**36**:7408−17.
288. Tanaka Y, Miyachi M, Kobuke Y. Selective vesicle formation from calixarenes by self-assembly. *Angew Chem Int Ed* 1999;**38**:504−6.
289. Zorzi RD, Guidolin N, Randaccio L, Purrello R, Geremia S. Nanoporous crystals of calixarene/porphyrin supramolecular complex functionalized by diffusion and coordination of metal ions. *J Am Chem Soc* 2009;**131**:2487−9.
290. Lee JW, Samal S, Selvapalam N, Kim HJ, Kim K. Cucurbituril homologues and derivatives: new opportunities in supramolecular chemistry. *Acc Chem Res* 2003;**36**:621−30.
291. Reany O, Li A, Yefet M, Gilson MK, Keinan E. Attractive interactions between heteroallenes and the cucurbituril portal. *J Am Chem Soc* 2017;**139**:8138−45.
292. Yang X, Wang R, Kermagoret A, Bardelang D. Oligomeric cucurbituril complexes: from peculiar assemblies to emerging applications. *Angew Chem Int Ed* 2020;**59**:21280−92.
293. Xue M, Yang Y, Chi X, Zhang Z, Huang F. Pillararenes, a new class of macrocycles for supramolecular chemistry. *Acc Chem Res* 2012;**45**:1294−308.
294. Kaizerman-Kane D, Hadar M, Tal N, Dobrovetsky R, Zafrani Y, Cohen Y. pH-Responsive pillar[6]arene-based water-soluble supramolecular hexagonal boxes. *Angew Chem Int Ed* 2019;**58**:5302−6.
295. Zhu H, Li Q, Gao Z, Wang H, Shi B, Wu Y, et al. Pillararene host-guest complexation induced chirality amplification: a new way to detect cryptochiral compounds. *Angew Chem Int Ed* 2020;**59**:10868−72.
296. Zhao YL, Stoddart JF. Azobenzene-based light-responsive hydrogel system. *Langmuir* 2009;**25**:8442−6.
297. Zhang X, Lei B, Wang Y, Xu S, Liu H. Dual-sensitive on-off switch in liposome bilayer for controllable drug release. *Langmuir* 2019;**35**:5213−20.
298. Liu H, Fu Y, Li Y, Ren Z, Li X, Han G, t al e. A fibrous localized drug delivery platform with NIR-triggered and optically monitored drug release. *Langmuir* 2016;**32**:9083−90.
299. Sarkar D, Chowdhury M, Das PK. Naphthalimide-based azo-functionalized supramolecular vesicle in hypoxia-responsive drug delivery. *Langmuir* 2022;**38**:3480−92.
300. Wang W, Lin L, Ma X, Wang B, Liu S, Yan X, et al. Light-induced hypoxia-triggered living nanocarriers for synergistic cancer therapy. *ACS Appl Mater Interfaces* 2018;**10**:19398−407.
301. Bian Q, Wang W, Wang S, Wang G. Light-triggered specific cancer cell release from cyclodextrin/azobenzene and aptamer-modified substrate. *ACS Appl Mater Interfaces* 2016;**8**:27360−7.
302. Long M, Liu X, Huang X, Lu M, Wu X, Weng L, et al. Alendronate-functionalized hypoxia-responsive polymeric micelles for targeted therapy of bone metastatic prostate cancer. *J Contr Release* 2021;**334**:303−17.
303. Joshi U, Filipczak N, Khan MM, Attia SA, Torchilin V. Hypoxia-sensitive micellar nanoparticles for co-delivery of siRNA and chemotherapeutics to overcome multi-drug resistance in tumor cells. *Int J Pharm* 2020;**590**:119915−29.
304. Zhang Y, Chan HF, Leong KW. Advanced materials and processing for drug delivery: the past and the future. Adv. *Drug Deliv Rev* 2013;**65**:104−20.
305. Zhou Y, Ye H, Chen Y, Zhu R, Yin L. Photoresponsive drug/gene delivery systems. *Biomacromolecules* 2018;**19**:1840−57.
306. Wang X, Sun B, Ye Z, Zhang W, Xu W, Gao S, et al. Enzyme-responsive COF-based thiol-targeting nanoinhibitor for curing bacterial infections. *ACS Appl Mater Interfaces* 2022;**34**:38483−96.
307. Zhu J, Guo T, Wang Z, Zhao Y. Triggered azobenzene-based prodrugs and drug delivery systems. *J Contr Release* 2022;**345**:475−93.

308. Ma X, Zhou N, Zhang T, Guo Z, Hu W, Zhu C, et al. In situ formation of multiple stimuli-responsive poly[(methyl vinyl ether)-alt-(maleic acid)] based supramolecular hydrogels by inclusion complexation between cyclodextrin and azobenzene. *RSC Adv* 2016;**6**:13129−36.
309. McConnell AJ, Wood CS, Neelakandan PP, Nitschke JR. Stimuli-responsive metal-ligand assemblies. *Chem Rev* 2015;**115**:7729−93.
310. Ma X, Tian H. Stimuli-responsive supramolecular polymers in aqueous solution. *Acc Chem Res* 2014;**47**:1971−81.
311. Kelley EG, Albert JNL, Sullivan, Epps TH. Stimuli-responsive copolymer solution and surface assemblies for biomedical applications. *Chem Soc Rev* 2013;**42**:7057−71.
312. Zhang K, Liu J, Guo Y, Li Y, Ma X, Lei Z. Synthesis of temperature, pH, light and dual-redox quintuple-stimuli-responsive shell-crosslinked polymeric nanoparticles for controlled release. *Mater Sci Eng C Mater Biol Appl* 2018;**87**:1−9.
313. Cheng W, Gu L, Ren W, Liu Y. Stimuli-responsive polymers for anticancer drug delivery. *Mater Sci Eng C Mater Biol Appl* 2014;**45**:600−8.
314. Razavi B, Abdollahi A, Roghani-Mamaqani H, Salami-Kalajahi M. Light- and temperature-responsive micellar carriers prepared by spiropyran-initiated atom transfer polymerization: investigation of photochromism kinetics, responsivities, and controlled release of doxorubicin. *Polymer* 2019;**187**:122046.
315. Chen S, Gao Y, Cao Z, Wu B, Wang L, Wang H, et al. Nanocomposites of spiropyran-functionalized polymers and upconversion nanoparticles for controlled release stimulated by near-infrared light and pH. *Macromolecules* 2016;**49**:7490−6.
316. Wang X, Liu X, Wang L, Tang CY, Law WC, Zhang G, et al. Synthesis of yolk-shell polymeric nanocapsules encapsulated with monodispersed upconversion nanoparticle for dual-responsive controlled drug release. *Macromolecules* 2018;**51**:10074−82.
317. Razavi B, Abdollahi A, Roghani-Mamaqani H, Salami-Kalajahi M. Light-, temperature-, and pH-responsive micellar assemblies of spiropyran-initiated amphiphilic block copolymers: kinetics of photochromism, responsiveness, and smart drug delivery. *Mater Sci Eng C* 2019;**109**:110524.
318. Lee H, Pietrasik J, Matyjaszewski K. Phototunable temperature-responsive molecular brushes prepared by ATRP. *Macromolecules* 2006;**39**:3914−20.
319. Zeinali E, Haddadi-Asl V, Roghani-Mamaqani H. Nanocrystalline cellulose grafted random copolymers of *N*-isopropylacrylamide and acrylic acid synthesized by RAFT polymerization: effect of different acrylic acid contents on LCST behavior. *RSC Adv* 2014;**4**:31428−42.
320. Haqani M, Roghani-Mamaqani H, Salami-Kalajahi M. Synthesis of dual-sensitive nanocrystalline cellulose-grafted block copolymers of *N*-isopropylacrylamide and acrylic acid by reversible addition-fragmentation chain transfer polymerization. *Cellulose* 2017;**24**:2241−54.
321. Hajebi S, Rabiee N, Bagherzadeh M, Ahmadi S, Rabiee M, Roghani-Mamaqani H, et al. Stimulus-responsive polymeric nanogels as smart drug delivery systems. *Acta Biomater* 2019;**92**:1−18.
322. Cheng CC, Muhabie AA, Huang SY, Wu CY, Gebeyehu BT, Lee AW, et al. Dual stimuli-responsive supramolecular boron nitride with tunable physical properties for controlled drug delivery. *Nanoscale* 2019;**11**:10393−401.
323. Zhang JG, Zhou ZH, Li L, Luo YL, Xu F, Chen Y. Dual-stimuli responsive supramolecular self-assemblies based on the host-guest interaction between β-cyclodextrin and azobenzene for cellular drug release. *Mol Pharm* 2020;**17**:1100−13.
324. Stubbs E, Laskowski E, Conor P, Heinze DA, Karis D, Glogowski EM. Control of pH- and temperature-responsive behavior of mPEG-*b*-PDMAEMA copolymers through polymer composition. *J Macromol Sci* 2017;**54**:228−35.
325. Shuai X, Ai H, Nasongkla N, Kim S, Gao J. Micellar carriers based on block copolymers of poly(q-caprolactone) and poly(ethylene glycol) for doxorubicin delivery. *J Contr Release* 2004;**98**:415−26.
326. Gao Z, Chen M, Hu Y, Dong S, Cui J, Hao J. Tunable assembly and disassembly of responsive supramolecular polymer brushes. *Polym Chem* 2017;**8**:2764−72.
327. Wataoka I, Urakawa H, Kajiwara K, Tsukahara Y. Molecular bottlebrushes. *Macromolecules* 1996;**29**:978−83.
328. Bhattacharya A, Misrab BN. Grafting: a versatile means to modify polymers−techniques, factors and applications. *Prog Polym Sci* 2004;**29**:767−814.
329. Müllner M, Dodds SJ, Nguyen TH, Senyschyn D, Porter CH, Boyd BJ, et al. Size and rigidity of cylindrical polymer brushes dictate long circulating properties *in vivo*. *ACS Nano* 2015;**9**:1294−304.
330. Blum AP, Kammeyer JK, Gianneschi NC. Activating peptides for cellular uptake *via* polymerization into high density brushes. *Chem Sci* 2016;**7**:989−94.
331. Liu GQ, Cai MR, Zhou F, Liu WM. Charged polymer brushes-grafted hollow silica nanoparticles as a novel promising material for simultaneous joint lubrication and treatment. *J Phys Chem B* 2014;**118**:4920−31.
332. Yu GC, Zhao R, Wu D, Zhang FW, Shao L, Zhou J, et al. Pillar[5]arene-based amphiphilic supramolecular brush copolymers: fabrication, controllable self-assembly and application in self-imaging targeted drug delivery. *Polym Chem* 2016;**7**:6178−88.
333. Miyake GM, Weitekamp RA, Piunova VA, Grubbs RH. Synthesis of isocyanate-based brush block copolymers and their rapid self-assembly to infrared-reflecting photonic crystals. *J Am Chem Soc* 2012;**134**:14249−54.
334. Song DP, Li C, Colella NS, Lu XM, Lee JH, Watkins JJ. Thermally tunable metallodielectric photonic crystals from the self-assembly of brush block copolymers and gold nanoparticles. *Adv Opt Mater* 2015;**3**:1169−75.
335. Macfarlane RJ, Kim B, Lee B, Weitekamp RA, Bates CM, Lee SF, et al. Improving brush polymer infrared one-dimensional photonic crystals *via* linear polymer additives. *J Am Chem Soc* 2014;**136**:17374−7.
336. Ballauff M, Borisov OV. Phase transitions in brushes of homopolymers. *Polymer* 2016;**98**:402−8.
337. Xiao W, Zeng X, Lin H, Han K, Jia HZ, Zhang XZ. Dual stimuli-responsive multi-drug delivery system for individual controlled release of anti-cancer drugs. *Chem Commun* 2015;**51**:1475−8.
338. San Miguel V, Bochet CG, Del Campo A. Wavelength-selective caged surfaces: how many functional levels are possible?. *J Am Chem Soc* 2011;**133**:5380−8.
339. Priestman MA, Sun L, Lawrence DS. Dual wavelength photoactivation of cAMP-and cGMP-dependent protein kinase signaling pathways. *ACS Chem Biol* 2011;**6**:377−84.
340. Rodrigues-Correia A, Weyel XMM, Heckel A. Four levels of wavelength-selective uncaging for oligonucleotides. *Org Lett* 2013;**15**:5500−3.
341. Scott TF, Kowalski BA, Sullivan AC, Bowman CN, McLeod RR. Two-color single-photon photoinitiation and photoinhibition for subdiffraction photolithography. *Science* 2009;**324**:913−7.
342. Wong PT, Tang S, Cannon J, Mukherjee J, Isham D, Gam K, et al. A thioacetal photocage designed for dual release: application in the quantitation of therapeutic release by synchronous reporter decaging. *Chembiochem* 2017;**18**:126−35.
343. Wong PT, Tang S, Cannon J, Chen D, Sun R, Lee J, et al. Photocontrolled release of doxorubicin conjugated through a thioacetal photocage in folate-targeted nanodelivery systems. *Bioconjugate Chem* 2017;**28**:3016−28.
344. Bochet CG. Orthogonal photolysis of protecting groups. *Angew Chem Int Ed* 2001;**40**:2071−3.
345. Kammari L, Solomek T, Ngoy BP, Heger D, Klan P. Orthogonal photocleavage of a monochromophoric linker. *J Am Chem Soc* 2010;**132**:11431−3.
346. Pelliccioli AP, Wirz J. Photoremovable protecting groups: reaction mechanisms and applications. *Photochem Photobiol Sci* 2002;**1**:441−58.

347. Banerjee A, Falvey DE. Protecting groups that can be removed through photochemical electron transfer: mechanistic and product studies on photosensitized release of carboxylates from phenacyl esters. *J Org Chem* 1997;**62**:6245−51.
348. Paul A, Bera M, Gupta P, Singh NDP. *o*-Hydroxycinnamate for sequential photouncaging of two different functional groups and its application in releasing cosmeceuticals. *Org Biomol Chem* 2019;**17**:7689−93.
349. He M, He G, Wang P, Jiang S, Jiao Z, Xi D, et al. A sequential dual-model strategy based on photoactivatable metallopolymer for on-demand release of photosensitizers and anticancer drugs. *Adv Sci* 2021;**8**:2103334−44.
350. Bio M, Nkepang G, You Y. Click and photo-unclick chemistry of aminoacrylate for visible light-triggered drug release. *Chem Commun* 2012;**48**:6517−9.
351. Van Dijken A, Bastiaansen JJAM, Kiggen NMM, Langeveld BMW, Rothe C, Monkman A, et al. Carbazole compounds as host materials for triplet emitters in organic light-emitting diodes: polymer hosts for high-efficiency light-emitting diodes. *J Am Chem Soc* 2004;**126**:7718−27.
352. Bashir M, Bano A, Ijaz AS, Chaudhary BA. Recent developments and biological activities of N-substituted carbazole derivatives: a review. *Molecules* 2015;**20**:13496−517.
353. Ameen S, Lee SB, Yoon SC, Lee J, Lee C. Diphenylaminocarbazoles by 1,8-functionalization of carbazole: materials and application to phosphorescent organic light-emitting diodes. *Dyes Pigments* 2016;**124**:35−44.
354. Venkatesh Y, Srivastava HK, Bhattacharya S, Mehra M, Datta PK, Bandyopadhyay S, et al. One- and two-photon uncaging: carbazole fused *o*-hydroxycinnamate platform for dual release of alcohols (same or different) with real-time monitoring. *Org Lett* 2018;**20**:2241−4.
355. Venkatesh Y, Rajesh Y, Karthik S, Chetan AC, Mandal M, Jana A, et al. Photocaging of single and dual (similar or different) carboxylic and amino acids by acetyl carbazole and its application as dual drug delivery in cancer therapy. *J Org Chem* 2016;**81**:11168−75.
356. Ferguson LR, Denny WA. The genetic toxicology of acridines. *Mutat Res* 1991;**258**:123−60.
357. Chen YY, Lukka PB, Joseph WR, Finlay GJ, Paxton JW, McKeage MJ, et al. Selective cellular uptake and retention of SN28049, a new DNA-binding topoisomerase II-directed antitumor agent. *Cancer Chemother Pharmacol* 2014;**74**:25−35.
358. Mitra P, Chakraborty PK, Saha P, Ray P, Basu S. Antibacterial efficacy of acridine derivatives conjugated with gold nanoparticles. *Int J Pharm* 2014;**473**:636−43.
359. Zawada Z, Safarík M, Dvoráková E, Janousková O, Brezinová A, Stibor I, et al. Quinacrine reactivity with prion proteins and prion-derived peptides. *Amino Acids* 2013;**44**:1279−92.
360. Belmont P, Bosson J, Godet T, Tiano M. Acridine and acridone derivatives, anticancer properties and synthetic methods: where are we now? *Anti Cancer Agents Med Chem* 2007;**7**:139−69.
361. Denny WA. Acridine derivatives as chemotherapeutic agents. *Curr Med Chem* 2002;**9**:1655−65.
362. Cholewinski G, Dzierzbicka K, Kołodziejczyk AM. Natural and synthetic acridines/acridones as antitumor agents: their biological activities and methods of synthesis. *Pharmacol Rep* 2011;**63**:305−36.
363. Zhuang HB, Tang WJ, Yu JY, Song QH. Acridin-9-ylmethoxycarbonyl (Amoc): a new photochemically removable protecting group for alcohols. *Chin J Chem* 2006;**24**:1465−8.
364. Jana A, Saha B, Karthik S, Barman S, Ikbal M, Ghosh SK, et al. Fluorescent Photoremovable precursors (acridin-9-ylmethyl)ester: synthesis, photophysical, photochemical and biological applications. *Photochem Photobiol Sci* 2013;**12**:1041−52.
365. Piloto AM, Hungerford G, Costa SPG, Goncalves MST. Acridinyl methyl esters as photoactive precursors in the release of neurotransmitter amino acids. *Photochem Photobiol Sci* 2013;**12**:339−47.
366. Ray S, Banerjee S, Singh AK, Ojha M, Mondal A, Singh NDP. Visible light-responsive delivery of two anticancer drugs using single-component fluorescent organic nanoparticles. *ACS Appl Nano Mater* 2022;**5**:7512−20.
367. Biswas S, Mengji R, Barman S, Vangala V, Jana A, Singh NDP. 'AIE + ESIPT' Assisted photorelease: fluorescent organic nanoparticles for dual anticancer drug delivery with real-time monitoring ability. *Chem Commun* 2018;**54**:168−71.
368. Jesus S, Schmutz M, Som C, Borchard G, Wick P, Borges O. Hazard assessment of polymeric nanobiomaterials for drug delivery: what can we learn from literature so far. *Front Bioeng Biotechnol* 2019;**7**:261−97.
369. Kohane DS, Langer R. Biocompatibility and drug delivery systems. *Chem Sci* 2010;**1**:441−6.
370. Ratjen L, Arrue L. Internal targeting and external control: phototriggered targeting in nanomedicine. *ChemMedChem* 2017;**12**:1908−16.
371. Abueva C. Photo-triggered theranostic nanoparticles in cancer therapy. *Med Lasers* 2021;**10**:7−14.